Phylogenomic incongruence gives new perspectives on the taxonomic complexity of Muscari s.l. (Asparagaceae, Scilloideae)

Hall, H. ORCID: https://orcid.org/0000-0002-3846-5802, Bilsborrow, J. ORCID: https://orcid.org/0000-0002-4404-9514, David, J. ORCID: https://orcid.org/0000-0003-0557-9886, Dizkirici, A. ORCID: https://orcid.org/0000-0002-0578-5092, Könyves, K. ORCID: https://orcid.org/0000-0002-8303-1544 and Culham, A. ORCID: https://orcid.org/0000-0002-7440-0133 (2025) Phylogenomic incongruence gives new perspectives on the taxonomic complexity of Muscari s.l. (Asparagaceae, Scilloideae). TAXON. tax.70002. ISSN 1996-8175 doi: 10.1002/tax.70002 Available at https://centaur.reading.ac.uk/124185/

RESEARCH ARTICLE

Phylogenomic incongruence gives new perspectives on the taxonomic complexity of *Muscari* s.l. (Asparagaceae, Scilloideae)

Hannah Hall,[1] Jordan Bilsborrow,[2] John David,[1,2] Ayten Dizkirici,[3] Kálmán Könyves[2] & Alastair Culham[1]

1 *Herbarium, Health & Life Sciences, School of Biological Sciences, University of Reading, Whiteknights, Reading, RG6 6EX, United Kingdom*
2 *Royal Horticultural Society, RHS Garden Wisley, Woking, GU23 6QB, United Kingdom*
3 *Department of Molecular Biology and Genetics, Van Yüzüncü Yıl University, 65080, Van, Türkiye*
Address for correspondence: *Alastair Culham, a.culham@reading.ac.uk*

DOI https://doi.org/10.1002/tax.70002

Abstract *Muscari* s.l. (Asparagaceae, Scilloideae) is a widespread genus of bulbous geophytes native to the Mediterranean, the Middle East and into the Caucasus. Based on inflorescence and floral morphology, four distinct groups have long been recognised and treated as either genera (*Muscari* s.str., *Muscarimia*, *Leopoldia*, *Pseudomuscari*) or subgenera within *Muscari* s.l. However, a recent molecular phylogenetic investigation proposed a new subgenus, *Pulchella*. Despite the several morphological and molecular phylogenetic investigations of *Muscari*, the delineation of taxa, either at the generic or subgeneric level, remains unstable. Here we aim to evaluate the monophyly and robustness of the recognised groups using broadly sampled nuclear (low-copy number and ribosomal cistron) and plastome sequence phylogenies of *Muscari* s.l. Our morphological and molecular delineation of *M.* subg. *Muscarimia* and subg. *Pseudomuscari* across the analyses of three data sources are broadly congruent. However, high levels of incongruence within *M.* subg. *Leopoldia* and subg. *Muscari* are reported and discussed here, with implications for the stability of the newly described *M.* subg. *Pulchella*. Nomenclatural rules also require a new subgenus name to replace the name *Pseudomuscari*, which is shown to be a synonym of subgenus *Muscari* and has therefore been misapplied in recent work.

Keywords Angiosperms353; conflict; grape hyacinth; nuclear; *Paramuscari*; *Pulchella*; taxonomy; whole plastome

Supporting Information may be found online in the Supporting Information section at the end of the article.

■ INTRODUCTION

Hyacinthinae Parl. (Asparagaceae, Scilloideae) encompasses over 300 species (Catalogue of Life, Bánki & al., 2025) of bulbous, mostly spring-flowering plants, distributed across Europe, the Middle East and Central Asia, with one outlier in Eastern Asia. Several species have a long history in horticulture, including the hyacinth, *Hyacinthus orientalis* L. At present, the subtribe comprises between 8 and 21 genera dependent on the treatment followed (Tutin & al., 1980; Speta, 1998).

Molecular studies that have included members of the subtribe have all recovered three main clades: Scilla, Fessia, and Hyacinthoides (Pfosser & Speta, 1999; Ali & al., 2012; Buerki & al., 2012); and have largely supported the morphological generic treatment by Speta (1998). These molecular studies have highlighted that some floral characteristics seem to have arisen through parallel evolution, such as the coherence or fusion of perianth segments to form a floral tube, which occurs in all three clades. This is in strong contrast to the usual stellate blue flowers that occur in most of the representatives of the subtribe. Within the Scilla clade, two genera have fused perianth segments: *Muscari* Mill. and *Bellevalia* Lapeyr. The two genera are separated morphologically based on the arrangement of the stamens, and this separation is further supported by the difference in base chromosome number (Speta, 1998) and molecular studies (Pfosser & Speta, 1999; Ali & al., 2012; Buerki & al., 2012, Böhnert & al., 2023, Roudsari & al., 2025).

Muscari s.l. includes 90 accepted species (suppl. Table S1), with new ones frequently being described (Doğu & Uysal, 2019; Eker, 2019a,b; Kayiran & al., 2019; Eker & al., 2020; Eker & Yildirim, 2021; Uysal & al., 2022; Alipour & al., 2024). These species are often grouped into four main inflorescence types (Fig. 1), and these groups can be treated as four distinct genera: *Muscari* (= *Botryanthus* Kunth), *Leopoldia* Parl., *Muscarimia* Kostel. ex Losinsk. (= *Muscari* sensu Kunth) and *Pseudomuscari* Garbari & Greuter, or alternatively treated as subgenera (Baker, 1871; Stuart, 1970; Davis & Stuart, 1980, 1984; Suárez-Santiago & Blanca, 2013; Böhnert & al., 2023).

Article history: Received: 6 Sep 2024 | returned for (first) revision: 30 Dec 2024 | (last) revision received: 4 Mar 2025 | accepted: 30 Apr 2025
Associate Editor: M. Montserrat Martinez-Ortega |

Muscari s.str. is characterised by a dense conical raceme of blue, black, or violet globose to oblong-urceolate flowers and an inconspicuous apical ring of sterile flowers (Fig. 1A). *Leopoldia* has brown, yellow, or green tubular to oblong urceolate fertile flowers and a top tassel of blue, violet, or pink sterile flowers on elongated pedicels (Fig. 1B). Species from both taxa are found throughout the Iberian Peninsula to the Middle East. *Muscarimia* is characterised by a dense and fleshy raceme of strongly scented pale pink to yellow and pale green narrow tubular flowers (Fig. 1C), thick and fleshy perennial roots (in comparison to the annual roots of all other *Muscari* s.l. species) and grows throughout southwest Turkey and the Aegean Islands. *Pseudomuscari* has lax to dense racemes of pale blue short to oblong campanulate fertile flowers (Fig. 1D), with species growing in Turkey, and throughout the Middle East and into the Caucasus, apart from *Muscari parviflorum* Desf., which has a Mediterranean distribution.

Pseudomuscari was formally recognised as a genus in 1970 by Garbari & Greuter (1970), when they grouped *Muscari* species with a non-constricted perianth and selected *P. azureum* (Fenzl) Garbari & Greuter (= *Muscari azureum* Fenzl) as the type. The list of accepted species for genus *Pseudomuscari* was published in separate works by Garbari (1970, 1973). The same year Stuart (1970) published *Pseudomuscari* as a subgenus within *Muscari*, typified with *M. pallens* (M.Bieb.) Fisch. While based on different types, the genus *Pseudomuscari* Garbari & Greuter and *M.* subg. *Pseudomuscari* D.C.Stuart comprise broadly the same set of recognised species (Stuart, 1970; Garbari, 1970, 1973). Davis & Stuart (1980) later treated *Muscari* in the broad sense (*Muscari* s.l.) using the subgenera *M.* subg. *Botryanthus* (Kunth) Rouy, subg. *Leopoldia* (Parl.) Peterm., subg. *Muscari* (= *Muscarimia* Kostel. ex Losinsk.), and subg. *Pseudomuscari*. However, in the *Flora of Turkey*, Davis & Stuart (1984) included all species of *M.* subg. *Pseudomuscari* in subg. *Botryanthus* with the comment that *Pseudomuscari* is a polyphyletic assemblage in need of further research, a point echoed in the work of Speta (1998).

Most phylogenetic studies that have included *Muscari* s.l. have been built upon a few commonly used plastid markers (including *matK*, *trnL-trnF*) and narrow taxon sampling often at a regional level and therefore do not cover the taxonomic or geographic breadth of the genus (Pfosser & Speta, 1999; Ali & al., 2012; Buerki & al., 2012; Dizkirici & al., 2019). Phylogenetic investigations based upon a single or few plastid genes can result in incongruent topologies between gene trees, low phylogenetic resolution, and inconsistent delineation of taxa (Gonçalves & al., 2019; Zhang & al., 2020; Liu & al., 2022), due to the varying evolutionary rate and selective pressure between the genes (Robbins & Kelly, 2023). Progress in high-throughput sequencing has enabled genome-scale data collection of uniparentally inherited whole organellar (chloroplast, mitochondria) and biparentally inherited nuclear loci (nuclear ribosomal cistron, nuclear genes) using methods such as whole genome skimming (Shi & al., 2012; Straub & al., 2012), ddRAD (Peterson & al., 2012), and targeted hybrid enrichment (Hyb-Seq) (Weitemier & al., 2014; Dodsworth & al., 2019). The addition of nuclear loci in phylogenetic inference, particularly when compared with chloroplast loci, allows for the identification of incongruence arising from hybridisation, introgression or incomplete lineage sorting (Twyford & Ennos, 2012; Folk & al., 2023; Stull & al., 2023).

Böhnert & al. (2023) provided the first broadly sampled chloroplast and double digest restriction-site associated

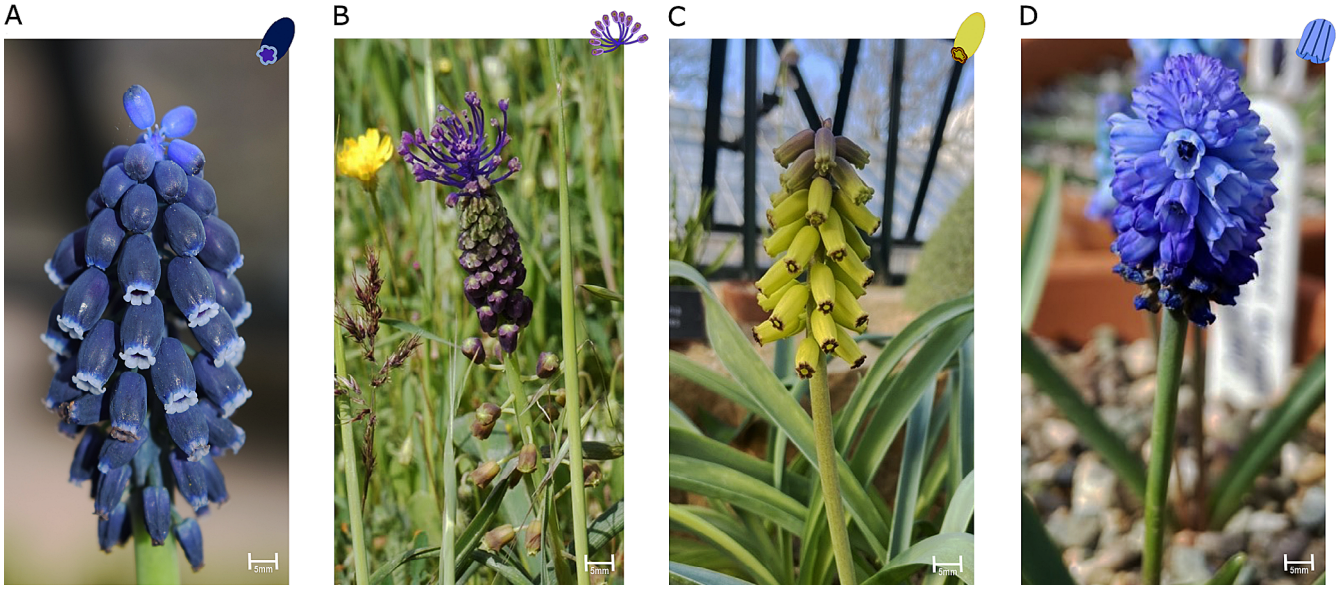

Fig. 1. Inflorescence types. **A**, *Muscari* (*M. neglectum* Guss. ex Ten.); **B**, *Leopoldia* (*M. comosum* (L.) Mill.); **C**, *Muscarimia* (*M. macrocarpum* Sweet); **D**, *Pseudomuscari* (*M. azureum* Fenzl). — Icons represent inflorescence types. Photos: A, John David; B–D, Hannah Hall.

DNA (ddRAD) phylogenetic study of *Muscari* s.l. Based upon the results of their ddRAD tree, they recognised a fifth subgenus, *M.* subg. *Pulchella* Böhnert, comprised of a clade containing *M. bourgaei* Baker, *M. kerkis* Karlén, *M. latifolium* J.Kirk, and the type, *M. pulchellum* Heldr. & Sartori ex Boiss., species all previously placed in *M.* subg. *Muscari* based upon morphological traits (Davis & Stuart, 1980; Karlén, 1984). However, in their plastid tree, *M.* subg. *Pulchella* is polyphyletic, with *M. pulchellum* sister to *M. kerkis*, which is in turn sister to *Leopoldia neumannii* Böhnert & Lobin (= *Muscari neumannii* (Böhnert & Lobin) Böhnert). Additionally, Böhnert & al. (2023) recovered a polyphyletic *M.* subg. *Pseudomuscari* in their ddRAD and chloroplast DNA tree resulting from the samples of *P. coeruleum* (Losinsk.) Garbari (= *Muscari coeruleum* Losinsk.) and *P. pallens* (M.Bieb.) Garbari (= *M. pallens* (M.Bieb.) Fisch.), clustering with members of *M.* subg. *Muscari*.

Despite the morphological and molecular investigations of *Muscari* s.l. to date, the delineation of taxa either at the generic or subgeneric level, remains unclear due to conflict of morphological and DNA-based classifications. Therefore, the aim of this study was to evaluate and test subgeneric delimitations within *Muscari* s.l. and explore the evolutionary processes underlying the observed phylogenetic patterns and diversity. To achieve this, we present the most comprehensive phylogenomic investigation of the genus, incorporating nuclear data (low-copy nuclear genes and nuclear ribosomal cistrons) and plastome data.

In this study, we decided to recognise *Muscari* in the broad sense (s.l.), treating *Muscari*, *Leopoldia*, *Muscarimia*, and *Pseudomuscari* at the subgeneric rank, as this approach enhances taxonomic stability and minimises taxonomic disruption (Nicolle & al., 2025). Although subgeneric boundaries may differ, the species binomials remain unchanged.

■ MATERIALS AND METHODS

Taxon sampling. — Leaf material of a total of 46 samples of *Muscari* s.l. and 6 samples of outgroup species were included in this study. Additionally, 28 samples of DNA were provided from the work of Dizkirici & al. (2019). In total, this investigation represents 41 out of the 90 (46%) currently recognised species of *Muscari* s.l. (Table 1 and suppl. Table S1). Sample information can be found in Appendix 1 and suppl. Table S7.

DNA extractions. — DNA was extracted from silica dried leaf material using the QIAGEN DNeasy Plant Mini Kit following the manufacturer's protocol (QIAGEN, Manchester, U.K.). Qubit Fluorometer (Thermo Fisher Scientific, Waltham, Massachusetts, U.S.A.), NanoDrop spectrophotometer (Thermo Fisher Scientific) and agarose gel electrophoresis were used to determine DNA quality and quantity.

Sequencing. — Library development and Illumina NovaSeq 6000 150bp PE (paired-end) sequencing for the genome skimming of all extracted DNA samples provided by Dizkirici & al. (2019) and DNA from five leaf samples (L_cyc1, M_gra, P_cha, S_mes1, S_sib1), were completed by Novogene (Cambridge, U.K.). The Dizkirici & al. (2019) and five additional samples were received and processed before access to the Angiosperms353 kit, thus only genome skimming data is available for these samples. The remaining samples were subjected to both genome skimming and enrichment using the Angiosperms353 probe kit (Johnson & al., 2019). The addition of Angiosperms353 enrichment was used to improve resolution and support.

Angiosperms353 library preparation, enrichment, genome skimming, and sequencing of the remaining samples were carried out by Daicel Arbor Biosciences (Ann Arbor, Michigan, U.S.A.) following the MyBaits protocol and were then pooled (70% captured and 30% non-captured). The final library pools were sequenced with Illumina NovaSeq 6000 S4 150bp PE at ~1Gb per sample.

Assemblies and annotations

Low-copy nuclear genes. — Raw paired-end sequence reads generated from the Angiosperms353 were trimmed using Trimmomatic v.0.39 (Bolger & al., 2014). HybPiper v.2 (Johnson & al., 2016) was used to assemble on-target nuclear genes from paired-end reads using the options BWA (Li & Durbin, 2009) and the Angiosperms353 mega353 target file filtered to "Monocots" (McLay & al., 2021). The command "--run_intronerate" was also used to assemble supercontigs (exons + introns). Summary statistics of gene recovery were produced using the hybpiper_stats script. Using the hybpiper_stats.tsv output, a custom R (v.4.3.2.) script (available at https://github.com/HannahRH98/Hyb-seq-Filtering/blob/main/filter_step1_samples.R) helped to guide decisions on the best sample filtering strategy, aiming to minimise the number of samples excluded. Any sample with less than 70% of genes was removed. Following sample filtering, using the hybpiper_recovery script, we recovered the target supercontig sequences. Using the seq_length.tsv output of the hybpiper_stats command, a custome R script (available at https://github.com/HannahRH98/Hyb-seq-Filtering/blob/main/filter_step2_genes.R) was used to guide decisions on the best gene filtering strategy. Any gene which was present in less than 70% of the samples was removed. Paralogs were detected using the HybPiper paralog_retriever script. All genes identified as paralogs were checked using the "Scenario One" tree method as described on the HybPiper wiki (https://github.com/mossmatters/HybPiper/wiki/Paralogs) (Method 1 in suppl. Appendix S1).

After filtering, three samples and 15 genes were removed from the dataset. From the 338 remaining genes, 54 were identified and confirmed as potential paralogs and were excluded from further analyses. Therefore, the final dataset consisted of 44 samples and 284 genes.

For later downstream phylogenetic analyses, supercontigs were aligned using MAFFT v.7 (Katoh & Standley, 2013) with the "–auto" option selected and trimmed using trimAl (Capella-Gutiérrez & al., 2009) with the "-gappyout" function to remove poorly aligned regions in the alignment.

Whole plastome. — Whole plastomes were assembled using GetOrganelle v.1.7.5 (Jin & al., 2020) and NOVOPlasty v.4.3.1 (Dierckxsens & al., 2017) with default settings. For NOVOPlasty assemblies, a *Hyacinthoides non-scripta* (L.) Chouard ex Rothm. *matK* gene (MK926167; De Vere & al., 2012) was used as the starting seed. Both sets of assemblies per sample were aligned using the MAFFT v.1.4.0 (Katoh & al., 2002) algorithm in Geneious Prime 2022.0.2 (https://www.geneious.com) and compared for any ambiguities (Method 2 in suppl. Appendix S1). Final plastome assemblies were annotated using both GeSeq (Tillich & al., 2017) with third-party annotators; ARAGORN v.1.2.38 (Laslett, 2004), tRNAscan-SE v.2.0.7 (Chan & al., 2021) and Chloë v.0.1.0 (https://chloe.plastid.org/annotate.html) also selected, and the "Annotate from" function in Geneious Prime. For annotation in Geneious Prime, the annotated plastome sequence of *Hyacinthoides non-scripta* (MN824434; Garnett & al., 2020) was used as a reference. All gene boundaries were manually checked against the *Hyacinthoides non-scripta* (MN824434) reference, and plastome maps were generated using OGDRAW v.1.3.1 (Greiner & al., 2019).

The final dataset consisted of 72 complete plastomes (68 *Muscari* s.l., 4 outgroups). For downstream phylogenomic analyses, one copy of the plastome inverted repeat (IR) was removed, and the plastomes were aligned using MAFFT v1.4.0 with the "–auto" option selected as implemented in Geneious Prime.

Protein-coding gene sequences. — Protein-coding gene sequences (CDS) were extracted from each of the whole plastomes using the "Tools/Extract annotations" function in Geneious Prime. All extracted CDS were then mapped to the extracted CDS of *Muscari comosum* (L.) Mill. (CMOM2OR) using the "Map to Reference" feature in Geneious Prime at Medium-Low/Fast sensitivity with no fine tuning. Duplicate CDS from the IR regions were removed to leave only one copy. Assembled CDS were aligned using MACSE v.2 (Ranwez & al., 2018) with default settings, which accounts for the underlying codon structure of protein coding nucleotide sequences and concatenated in Geneious Prime prior to further analyses. The final dataset consisted of 78 CDS and 72 samples (68 *Muscari* s.l., 4 outgroups).

We have also run a combined plastid tree, which incorporates both our data and that of Böhnert & al. (2023) (Method 3 in suppl. Appendix S1, and suppl. Fig. S8).

Nuclear ribosomal cistron. — Assembly of the nuclear ribosomal cistrons initially used GetOrganelle with the partial sequence of a *Prospero autumnale* (L.) Speta nuclear ribosomal cistron (KC899300; Jang & al., 2013) as starting seed. Most samples failed to assemble into a single contig. We then used the longest assembled cistron contig, *Muscari coeleste* Fomin (M20_1), as a reference to assemble all samples in Geneious Prime using the "Map to Reference" feature with Medium-Low/Fast sensitivity and five iterations. All nuclear ribosomal cistron assemblies were annotated in Geneious Prime using the complete nuclear ribosomal cistron sequence of *Allium cepa* L. (KM117265) as reference and manually trimmed at the 5′-end of 18S and 3′-end of 26S genes to remove the areas which were difficult to align. The final dataset consisted of 72 nuclear ribosomal cistrons (68 *Muscari* s.l., 4 outgroups) and were aligned using MUSCLE v.3.8.425 (Edgar, 2004) with default settings as implemented in Geneious Prime, for later downstream phylogenomic analysis.

Phylogenetic analyses

Nuclear maximum likelihood supermatrix estimation. — Supercontig alignments were concatenated using AMAS (Borowiec, 2016) to generate a supermatrix alignment. Maximum likelihood (ML) analysis of the concatenated nuclear gene alignment was undertaken using IQ-TREE v.2.1.2 (Minh & al., 2020a). The alignment was partitioned by gene and the best-fitting models were determined by ModelFinder (Kalyaanamoorthy & al., 2017) using the "-m TESTMERGE" function under the Bayesian information criterion (BIC) as implemented in IQ-TREE (suppl. Table S2.). Branch support was

Table 1. Overview of subgenus-level coverage in this study of *Muscari* s.l. The table summarises the number of accepted species per subgenus (suppl. Table S1), the species included in this study, and the percentage of species covered within each subgenus. The number of accepted species and percentages may change by the time of publication due to newly described species added since the manuscript was written. The subgenus name *Pseudomuscari* is sensu Stuart (1970).

Subgenus	Accepted species	Species included in study	Species covered in this study (%)
Muscari s.str.	47	*Muscari adilii, M. alpanicum, M. anatolicum, M. armeniacum, M. atlanticum, M. aucheri, M. bourgaei, M. commutatum, M. discolor, M. grandifolium, M. kerkis, M. latifolium, M. macbeathianum, M. microstomum, M. neglectum, M. olivetorum, M. sandrasicum, M. serpentinicum, M. sivrihisardaghlarense, M. turcicum, M. vuralii*	45
Leopoldia	29	*Muscari babachii, M. caucasicum, M. comosum, M. cycladicum, M. erdalii, M. longipes M. massayanum, M. massayanum* (cf. *erzincanicum*), *M. matritense, M. mirum, M. spreitzenhoferi, M. tenuiflorum, M. weissii*	45
Pseudomuscari	7	*Muscari azureum, M. coeleste, M. inconstrictum, M. parviflorum, M. pseudomuscari*	71
Muscarimia	2	*Muscari macrocarpum, M. racemosum*	100
Unplaced	5	N/A	0

assessed with the SH-like approximate likelihood ratio test (SH-aLRT) (Guindon & al., 2010) set at 1000 replicates and 1000 ultra-fast bootstrap replicates (UFBoot) (Hoang & al., 2018).

Nuclear multispecies coalescent species tree estimation. — Using IQ-TREE, individual nuclear gene trees were generated from the supercontig alignments, with the best model of substitution for each alignment selected by ModelFinder. Branch support was assessed with SH-aLRT set at 1000 replicates and a 1000 ultra-fast bootstrap replicates. All gene trees were concatenated into a single treefile. Weakly supported branches (≤10% SH-aLRT) were collapsed using Newick Utilities v.1.6. (Junier & Zdobnov, 2010) and long branches were removed using TreeShrink v.1.3.9 (Mai & Mirarab, 2018). A species tree was inferred from the nuclear gene trees using the multispecies coalescent approach (MSC) ASTRAL-III v.5.7.8, with default settings (Zhang & al., 2018). Local posterior probabilities (LPP) were calculated as branch support measures (Sayyari & Mirarab, 2016).

Nuclear concordance scores. — We calculated gene and site concordance factor scores (gCF, sCF) across the ASTRAL species tree as implemented in IQ-TREE (Minh & al., 2020b). The gCF is the percentage of gene trees containing a particular branch while sCF is the percentage of alignment sites supporting a particular branch in the species tree. We also used the normalised quartet score as implemented in ASTRAL-III, to identify the number of the total gene quartet trees agreed with the overall species tree.

Species networks. — NANUQ (Allman & al., 2019) as implemented in MSCquartets v.3 R package (Rhodes & al., 2021; Allman & al., 2024) was used to estimate a species network of *Muscari* s.l. and to visualise introgressive gene flow between taxa while accounting for incomplete lineage sorting. As input, we took the nuclear gene trees as generated for the MSC species tree estimation, but with outgroups removed, and set the alpha to 1e-06 and the beta to 0.95 (Allman & al., 2019). To visualise the final network, we used SplitsTree v.6 (Huson, 1998; Huson & Bryant, 2024) with default parameters.

Plastome and nuclear ribosomal cistron. — ML and Bayesian inference (BI) methods were run for the plastome, concatenated CDS, and nuclear ribosomal cistron datasets. ML analyses were undertaken using IQ-TREE. The plastome and nrDNA alignments were treated as unpartitioned datasets while the CDS was partitioned under the gene-by-codon partitioning scheme. The best-fitting model was selected by ModelFinder under the BIC criterion as implemented in IQ-TREE. For the plastome alignment, the best model was K3Pu + F + R4, and for the nuclear ribosomal cistron alignment it was GTR + F + I + Γ4. For the partitioned concatenated CDS alignment, the best models can be found in suppl. Table S3. Branch support was assessed with SH-aLRT set at 1000 replicates and a 1000 ultra-fast bootstrap replicates.

BI analyses were undertaken using MrBayes v.3.2.7 (Ronquist & al., 2012) with two separate runs, each of four chains, run for five million generations and sampled every 1000 generations. For the plastome and the nuclear ribosomal cistron alignments, the best model of nucleotide substitution was determined using jModelTest v.2 (Darriba & al., 2012) under the BIC and limited to those compatible with MrBayes. For the partitioned concatenated CDS alignment, the best model of nucleotide substitution was determined by ModelFinder under the BIC as implemented in IQ-TREE using the "-m TESTMERGEONLY" function with model selection limited to those compatible with MrBayes. The best model of nucleotide substitution for the plastome and nuclear ribosomal cistron datasets was set to GTR + I + Γ. The best models for the CDS dataset can be found in suppl. Table S4. Tracer v.1.7.2 (Rambaut & al., 2018) was used to assess the quality of the Markov chain Monte Carlo simulations and stability of runs. The first 25% of trees were discarded as burn-in and the remaining trees were used to construct extended majority-rule consensus trees with the "allcompat" option in MrBayes. Branch support was assessed with posterior probability (PP).

All phylogenetic trees were visualised in FigTree v.1.4.4 (http://tree.bio.ed.ac.uk/software/figtree/) and annotated in Inkscape v.1.2.1 (https://inkscape.org/).

■ RESULTS

Low-copy nuclear genes. — We recovered an average of 7,833,554 reads per sample, with a minimum of 1,308,616 (*Muscari neglectum* Guss. ex Ten. & Sangiov., MNEGLR) and a maximum of 20,740,590 reads (*M. mirum* Speta, MMIRUM). Percentage of reads that mapped to sequences in the filtered mega353 gene target file was on average 7.94%, with a minimum of 1.9% (*M. mirum*, MMIRUM) and a maximum of 23.8% (*M. neglectum*, MNEGIR) (suppl. Table S5).

After alignment and trimming, supercontig alignment length on average was 1703 bp with a minimum of 208 bp (gene 6048) and maximum of 5891 bp (gene 6320). The average percentage of missing data in the alignment was 7.93% with a minimum of 0.396% (gene 5960) and maximum of 59.772% (gene 5968) (suppl. Table S6).

The final nuclear supercontig alignment used for the supermatrix ML phylogenetic analyses was 483,561 bp (suppl. Appendix S2) with a tree length of 1.2506 as calculated in IQ-TREE. Tree length is the measure of a genes' evolutionary rate. Along with alignment length, it represents a complementary measure of a genes' or alignment's information content (Walker & al., 2019).

Whole-plastome structure. — The shortest *Muscari* s.l. whole plastome was 152,977 bp (*Muscari turcicum* Uysal & al., M27_1) (Fig. 2) and the longest was 155,764 bp (*M. racemosum* Mill. M.mus) (Fig. 3). All *Muscari* s.l. species show the canonical quadripartite structure, with a large single-copy (LSC) region (82,406–84,058 bp), a small single copy (SSC) region (18,163–18,528 bp) separated by two inverted repeats (IR_A and IR_B) (26,024–26,798 bp) (suppl. Table S7). All *Muscari* s.l. whole plastomes had a typical GC content of between 37.6% and 37.7%. While *Muscari* s.l. plastomes show limited variation overall, differences in

plastome length primarily come from intergenic spacers located in the LSC. The final plastome alignment (with one copy of the IR removed) included 72 samples and was 136,104 bp long (suppl. Appendix S3) with a tree length of 0.1208 as calculated in IQ-TREE.

Plastomes with one IR removed contained between 77 (*M. turcicum*, M27_1) to 79 (*M. mirum*, M34_2 and MMIRUM) CDS. The translation initiation factor, *infA* was excluded from further analysis due to a 7 bp insertion resulting in a premature stop codon in 70 samples. Only

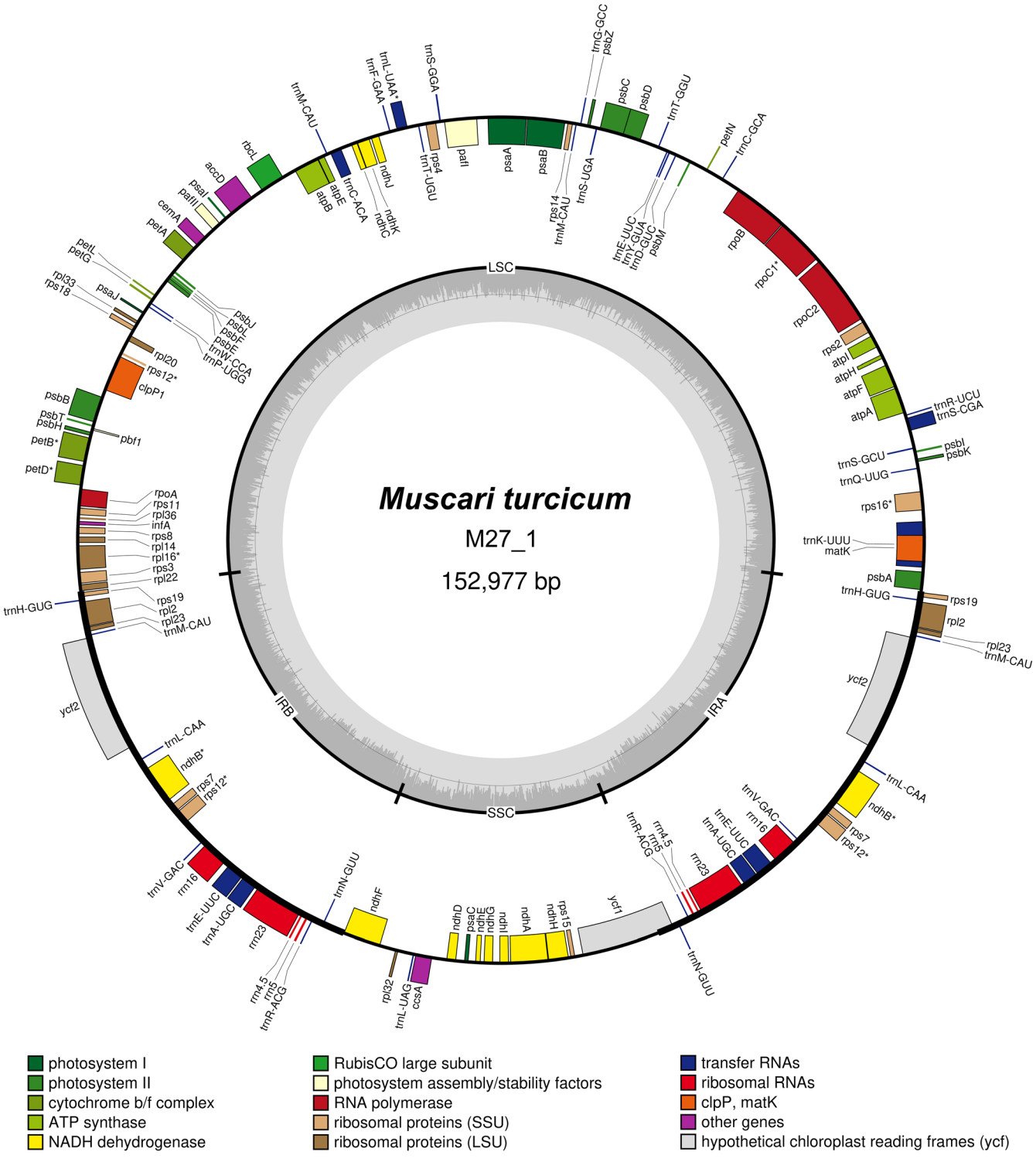

Fig. 2. Whole plastome of *Muscari turcicum*, the shortest plastome sampled. The outer circle shows positions of genes and the large single copy (LSC), small single copy (SSC), and two inverted repeat (IR_A and IR_B) regions. The inner circle graph shows GC content across the genome.

the two *Muscari mirum* samples had a functional *infA* gene. In contrast, only one species, *M. turcicum*, had *ndhF* classified as a putative pseudogene, resulting from a premature stop codon caused by a frameshift mutation of a 1 bp deletion. The *ndhF* gene was kept for the phylogenetic analyses. The concatenated 78 CDS alignment was 68,847 bp long (suppl. Appendix S4) with a tree length of 0.0755.

Nuclear ribosomal cistron. — Untrimmed nuclear ribosomal cistrons ranged in length from 10,268 bp (*Muscari aucheri* (Boiss.) Baker, MAUCH) to 11,636 bp (*M. coeleste*, M20_1)

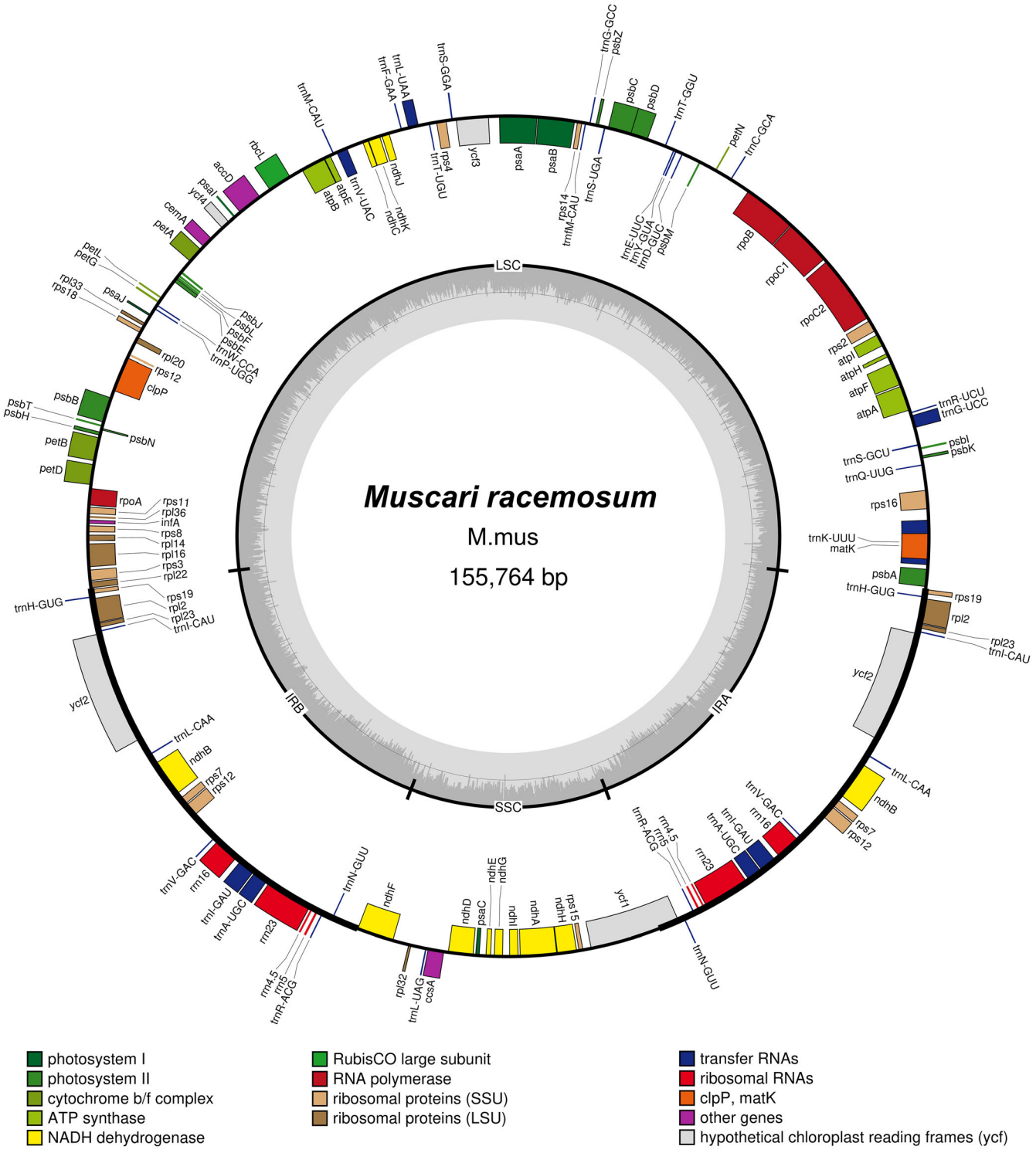

Fig. 3. Whole plastome of *Muscari racemosum*, the longest plastome sampled. The outer circle shows positions of genes and the large single copy (LSC), small single copy (SSC), and two inverted repeat (IR_A and IR_B) regions. The inner circle graph shows GC content across the genome.

(suppl. Table S7). The final trimmed nrDNA alignment was 5,934 bp long (suppl. Appendix S5) with a tree length of 0.1737.

Phylogenomic analyses of *Muscari* s.l. — Throughout all analyses, *Muscari* s.l. is recovered as a monophyletic group. For the low-copy nuclear gene dataset, the MSC (Fig. 4) and ML (suppl. Fig. S1) analyses produced broadly congruent topologies. The only major difference between the analyses is that in the MSC tree, *M.* subg. *Muscarimia* (Muscarimia clade) is recovered as sister to the Muscari N2 clade, subg. *Leopoldia* (Leopoldia clade), and Muscari N1 clade (Fig. 4), whereas in the ML tree, it is recovered as sister only to the Muscari N2 clade and subg. *Leopoldia* (Leopoldia clade) (suppl. Fig. S1). For the plastome dataset, the BI (Fig. 5) and ML (suppl. Fig. S2) analyses produced broadly congruent topologies. The only major difference is that in the BI tree, *Muscari mirum* (Leopoldia P3 clade) was recovered as sister to the Muscari P3 clade, and in the ML tree, *M. mirum* (Leopoldia P3 clade) and *M. commutatum* Guss. (Muscari P4 clade) were recovered as sister to each other, and in turn sister to the Muscari P3 clade. For the nuclear ribosomal dataset, BI (Fig. 6) and ML analyses (suppl. Fig. S3) produced broadly congruent topologies. Both the BI and ML CDS analyses (suppl. Figs. S4, S5) produced broadly congruent topologies to the plastome BI tree.

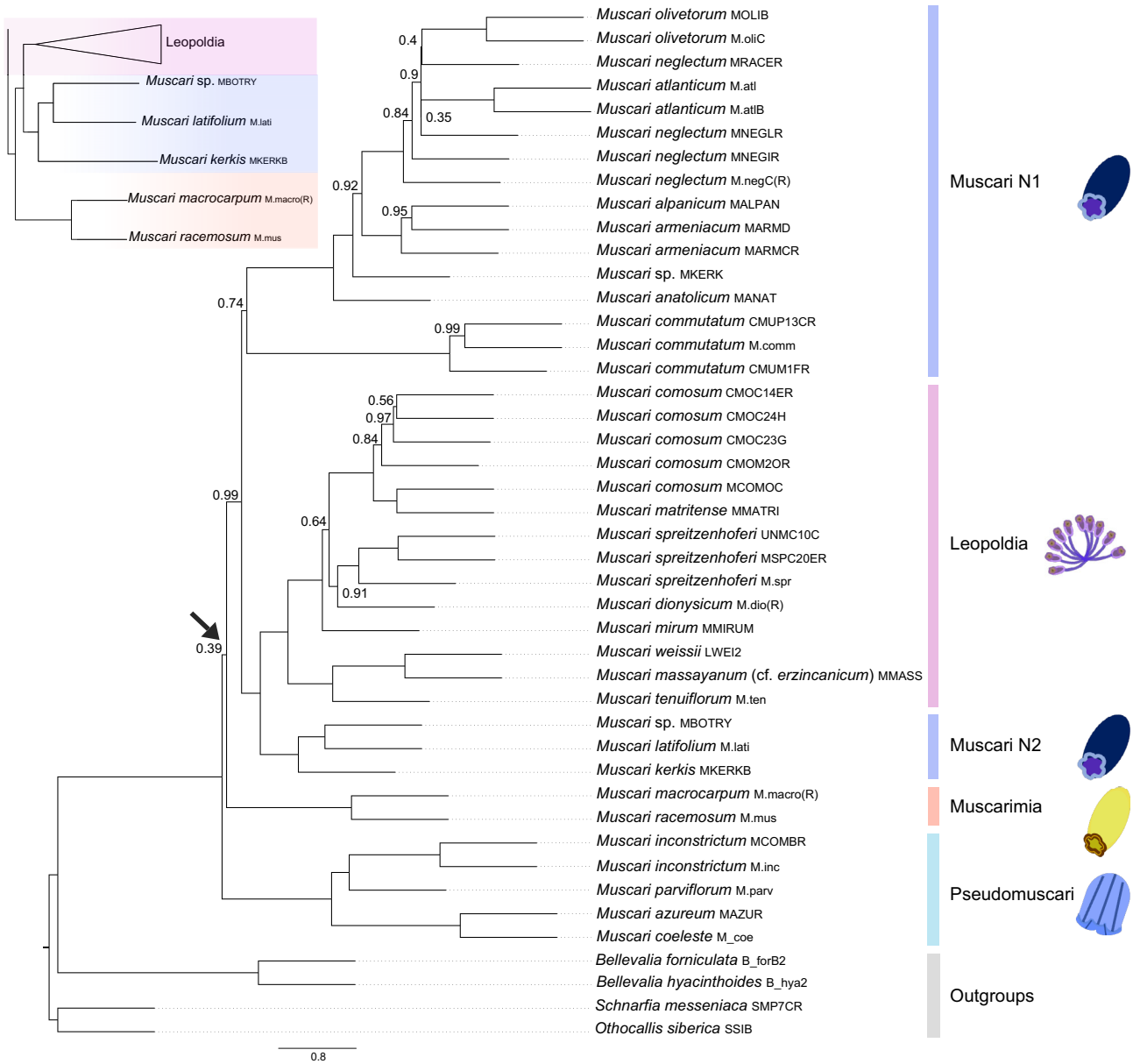

Fig. 4. MSC ASTRAL phylogenetic tree based on 284 newly generated low-copy nuclear genes of 40 *Muscari* s.l. samples and 4 outgroups. Only support values below 1.0 local posterior probability are shown. Scale bar in coalescent units. Sample codes correspond to those in Appendix 1. Colour of the bars indicates subgenera. Icons represent inflorescence types as in Fig. 1. Arrow indicates the incongruent branch between the ML and MSC phylogenetic trees as shown in the inset panel.

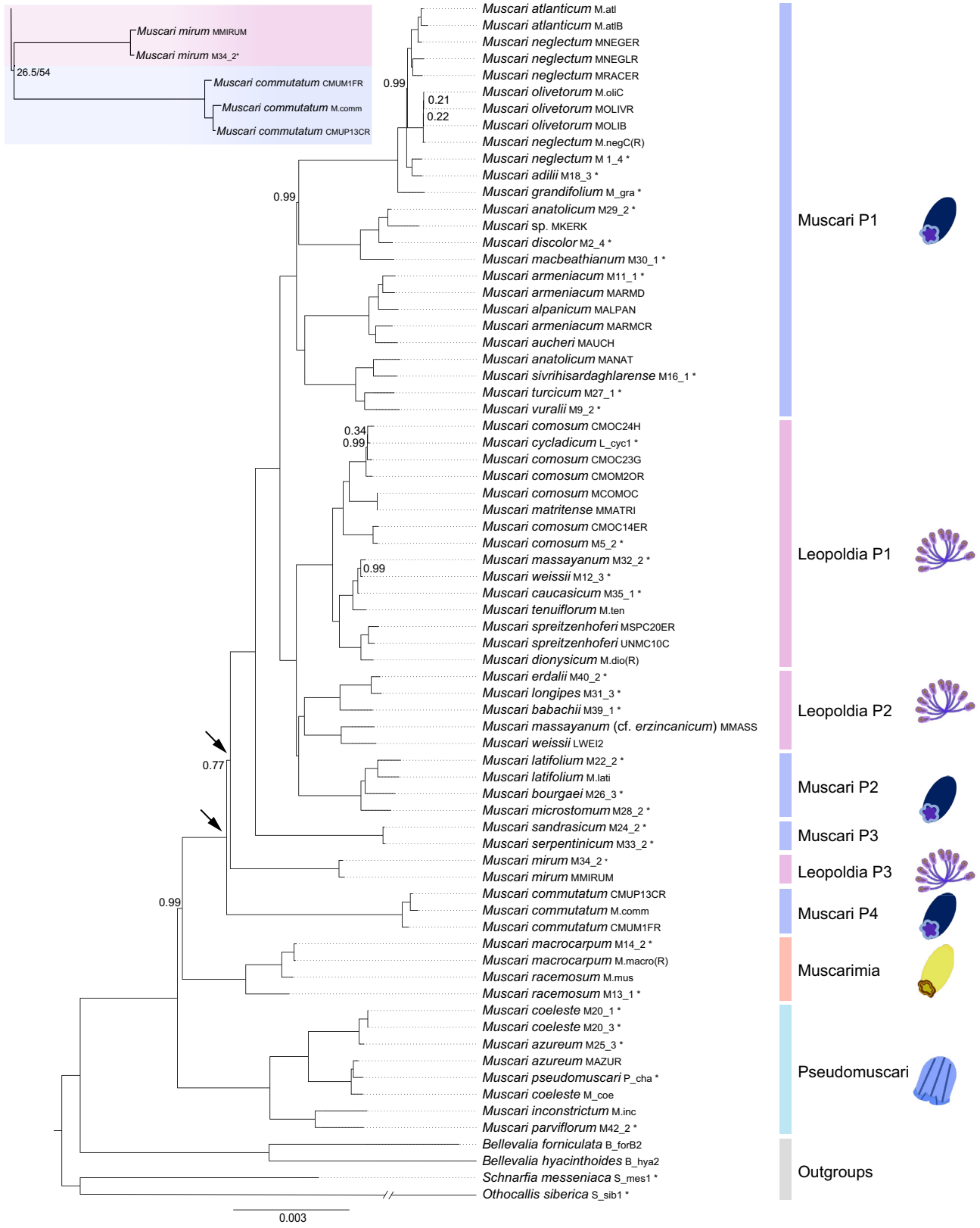

Fig. 5. Bayesian phylogenetic tree based on 68 newly generated plastome sequences of *Muscari* s.l. and 4 outgroup species. Only branch support values below 1.0 posterior probability are shown. Scale bar shows the number of substitutions per site. Sample codes correspond to those in Appendix 1. Colour of the bars indicates subgenera. Icons represent inflorescence types as in Fig 1. // indicates that the branch has been shortened. Arrows indicate incongruent branches between the ML and the BI phylogenetic trees as shown in the inset panel. Asterisk (*) denotes that sample was genome skimmed only.

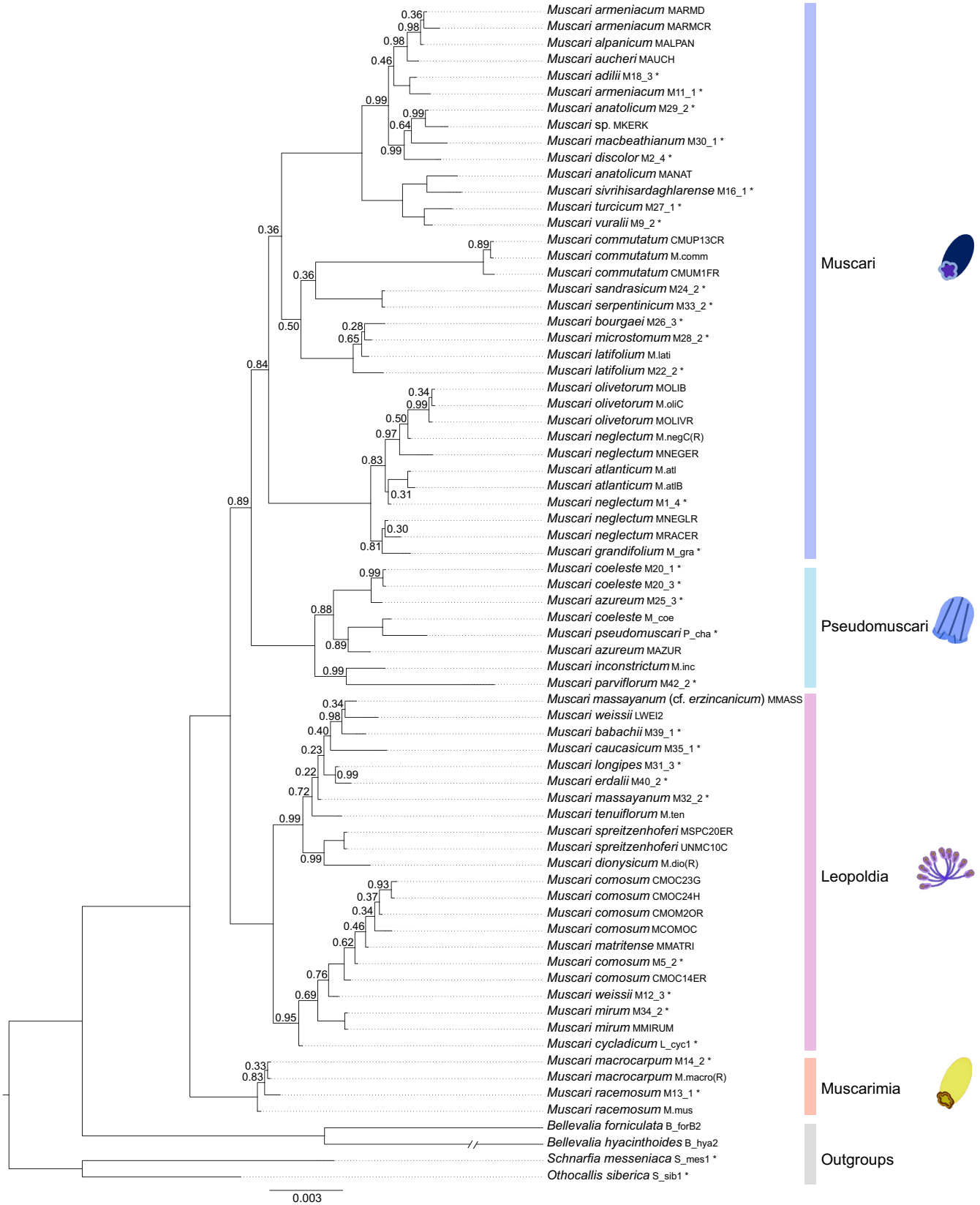

Fig. 6. Bayesian phylogenetic tree based on 68 newly generated nuclear ribosomal cistron sequences of *Muscari* s.l. and four outgroup species. Only branch support values below 1.0 posterior probability are shown. Scale bar shows the number of substitutions per site. Sample codes correspond to those in Appendix 1. Colour of the bars indicates subgenera. Icons represent inflorescence types as in Fig. 1. // indicates that the branch has been shortened. Asterisk (*) denotes that sample was genome skimmed only.

Therefore, only the MSC low-copy nuclear gene, BI plastome and BI nuclear ribosomal cistron analyses are shown here. However, branch support reported in the text shows support values across analyses (including ML) for the respective branches (ASTRAL local posterior probabilities [LPP], Bayesian inference posterior probabilities [PP], and maximum likelihood analyses SH-aLRT and UFBoot).

When multiple samples of one species were used, these samples largely grouped regardless of whether they were sequenced by Novogene or Daicel Arbor Biosciences, and we did not detect any systemic sequencing bias correlated with the two different service suppliers.

***Muscari* subg. *Muscarimia* and subg. *Pseudomuscari*. —** *Muscari* subg. *Pseudomuscari* (Pseudomuscari clade) and subg. *Muscarimia* (Muscarimia clade) were recovered as monophyletic in all analyses (1.00 LPP, 1.00 PP, 100% SH-aLRT, 100% UFBoot) (Figs. 4, 5, 6, and suppl. Figs. S1, S2, S3). However, the placement of the clades change, with *M.* subg. *Pseudomuscari* (Pseudomuscari clade) being sister to the rest of *Muscari* s.l. in the low-copy nuclear gene analysis (1.00 LPP, 100% SH-aLRT, 100% UFBoot) (Fig. 4, and suppl. Figs. S1) and plastome analysis (1.00 PP, 100% SH-aLRT, 100% UFBoot) (Fig. 5, suppl. Fig. 2), but sister to *M.* subg. *Muscari* (Muscari clade) in the nuclear ribosomal cistron analysis (0.89 PP, 85.9% SH-aLRT, 69.0% UFBoot) (Figs. 6, suppl. Fig. S3). Instead, *M.* subg. *Muscarimia* is recovered as sister to the rest of *Muscari* s.l. in the nuclear ribosomal cistron analysis (1.00 PP, 98.2% SH-aLRT, 100% UFBoot).

***Muscari* subg. *Leopoldia* and subg. *Muscari*. —** In the low-copy nuclear gene analyses (Fig. 4, suppl. Fig. S1), *Muscari* subg. *Leopoldia* (Leopoldia clade) is recovered as monophyletic (1.00 LLP, 100% SH-aLRT, 100% UFBoot). However, *M.* subg. *Muscari* is recovered as paraphyletic, with the Muscari N2 clade, containing species *M. latifolium*, *M. kerkis* and an unidentified *Muscari* sp., recovered as sister to *M.* subg. *Leopoldia* (Leopoldia clade) (1.00 LPP, 100% SH-aLRT, 100% UFBoot). *Muscari commutatum* is recovered in Muscari N1 but as sister to the rest of that clade (0.74 LPP, 100% SH-aLRT, 100% UFBoot) (Fig. 4, suppl. Fig. S1).

In the plastome tree (Fig. 5, suppl. Fig. S2) both *Muscari* subg. *Leopoldia* (Leopoldia P1, P2, and P3 clades) and subg. *Muscari* (Muscari P1, P2, P3, and P4 clades) are recovered as paraphyletic. *Muscari commutatum* (Muscari P4 clade) unlike in the MSC nuclear tree, is recovered as sister to *M. mirum* (Leopoldia P3 clade) (1.00 PP) (apart from in the ML analysis in which they are sister to each other; 26.5% SH-aLRT, 54.0% UFBoot) (Fig. 5, suppl. Fig. S2) which is in turn sister to *M. serpentinicum* Yıldırım & al. and *M. sandrasicum* Karlén (Muscari P3 clade) (0.77 PP, 100% SH-aLRT, 100% UFBoot). Furthermore, like the Muscari N2 clade, a smaller clade of the *M.* subg. *Muscari* species *M. latifolium*, *M. bourgaei*, and *M. microstomum* P.H.Davis & D.C.Stuart formed the Muscari P2 clade, which was strongly supported as sister to the Leopoldia P2 clade (1.00 PP, 91.3% SH-aLRT, 98.0% UFBoot) (Fig. 5, suppl. Fig. S2).

In the nuclear ribosomal cistron tree (Fig. 6, suppl. Fig. S3), both *Muscari* subg. *Muscari* (Muscari clade) and subg. *Leopoldia* (Leopoldia clade) were recovered as monophyletic with moderate (0.84 PP, 82.6% SH-aLRT, 65.0% UFBoot) and high support (1.00 PP, 96.8% SH-aLRT, 100% UFBoot), respectively.

In *Muscari* subg. *Leopoldia*, *M. matritense* Ruíz Rejón & al. (MMATRI) was recovered either sister to (Fig. 4) or nested within the *M. comosum* samples (Figs. 5, 6). Additionally, samples received as *M. massayanum* C.Grunert (M32_2 and MMASS) and *M. weissii* Freyn (M12_3 and LWEI2), also in *M.* subg. *Leopoldia*, are recovered as polyphyletic in both the plastome and nuclear ribosomal cistron analyses (Figs. 5, 6). *Muscari massayanum* and *M. weissii* samples M32_2 and M12_3 were not part of the low-copy nuclear gene analysis. The sample received as *M. dionysicum* Rech.f. (M.dio(R)) was recovered sister to *M. spreitzenhoferi* (Heldr. ex Osterm.) H.R.Wehrh. samples in all analyses (Figs. 4, 5, 6).

Within *Muscari* subg. *Muscari*, all three analyses (Figs. 4, 5, 6) recovered a clade including *M. atlanticum* Boiss. & Reut., *M. neglectum*, and *M. olivetorum* Blanca & al.

Nuclear gene tree and site concordance. — The normalised quartet scores as calculated by ASTRAL for the nuclear species tree was 0.68 indicating that a total of 68% of gene tree quartets agreed with the overall species tree. Nuclear gene tree and site concordance across the species tree was low, but prominent in *M.* subg. *Leopoldia* (Leopoldia clade) and subg. *Muscari* (Muscari N1 and N2 clades). However, regardless of gCF or sCF, most LPP were high with 63% of branches receiving a score of 1.00 LPP (suppl. Figs. S6, S7).

Species networks. — The NANUQ network was highly consistent with the 284-nuclear-gene ASTRAL tree and gene flow is reported both within and across clades to varying degrees (Fig. 7). While the Muscari N2 clade is recovered as sister to *Muscari* subg. *Leopoldia* (Leopoldia clade) in the low-copy nuclear gene species tree (Fig. 4), NANUQ revealed substantial levels of gene flow between the Muscari N2 clade, and *M.* subg. *Muscarimia* (Muscarimia clade) and subg. *Pseudomuscari* (Pseudomuscari clade). Gene flow between *M.* subg. *Leopoldia* (Leopoldia clade) and the Muscari N2 clade appears minimal. The Muscari N1 clade also exhibited minimal gene flow with other clades.

■ DISCUSSION

***Muscari* s.l. phylogeny. —** *Muscari* s.l. and *M.* subg. *Muscarimia* (Muscarimia clade) are monophyletic in all our analyses, although the placement of *M.* subg. *Muscarimia* varies, consistent with the previous findings of Dizkirici & al. (2019), and Böhnert & al. (2023). Our nuclear ribosomal cistron analysis recovers all four subgenera as monophyletic (Fig. 6). However, our two other datasets, low-copy nuclear genes and plastome, conflict with this latter finding.

***Muscari* subg. *Pseudomuscari*. —** Our data consistently support a monophyletic *Muscari* subg. *Pseudomuscari*

(Pseudomuscari clade) (Figs. 4, 5, 6), as did Dizkirici & al. (2019). However, our sampling did not include *M. pallens* and *M. coeruleum*, species that Böhnert & al. (2023) found to fall within *M.* subg. *Muscari*, resulting in a polyphyletic *M.* subg. *Pseudomuscari*.

The placement of *Muscari pallens* within *M.* subg. *Muscari* as reported by Böhnert & al. (2023) and in the combined analysis presented in suppl. Fig. S8 (Method 3 and Result 1 in suppl. Appendix S1), raises a question over the nomenclatural status of *M.* subg. *Pseudomuscari* as delineated by Stuart (1970), which is addressed later in this paper.

The autumn flowering *Muscari parviflorum* has traditionally been placed in *M.* subg. *Muscari* based upon constriction of the perianth (= *Muscari* s.str. Garbari & Greuter, 1970) but was later moved to *M.* subg. *Pseudomuscari* based karyological similarities (Stuart, 1970). Molecular data presented here support this inclusion of *M. parviflorum*, as do Dizkirici & al. (2019) and Böhnert & al. (2023).

***Muscari* subg. *Leopoldia* and subg. *Muscari*. —** Our low-copy nuclear gene and plastome analyses recover *Muscari* subg. *Muscari* as paraphyletic (Figs. 4, 5) as did Böhnert & al. (2023). However, Dizkirici & al. (2019) recovered a monophyletic *M.* subg. *Muscari* but this was likely due to taxon sampling limits. *Muscari* subg. *Leopoldia*, in contrast, is monophyletic in our low-copy nuclear gene analysis (Leopoldia clade) but paraphyletic in the plastome analysis (Leopoldia P1, P2, and P3). This is broadly congruent with the ddRAD data (assuming they are predominantly nuclear) and plastid findings of Böhnert & al. (2023). Dizkirici & al. (2019) also recovered a paraphyletic *M.* subg. *Leopoldia*.

In both the low-copy nuclear gene and plastome analyses, a second *Muscari* subg. *Muscari* clade (Muscari N2 and P2) was recovered as sister to *M.* subg. *Leopoldia* (Leopoldia clade, Fig 4.) or the Leopoldia P2 clade (Fig. 5) respectively. The Muscari N2 and P2 clades always included *M. latifolium*, but other species recovered within these clades varied due to different sampling across the analyses. Regardless, the Muscari N2 and P2 clades are broadly congruent with the plastid and ddRAD findings of Böhnert & al. (2023). Based upon the results of their ddRAD analysis, they describe this clade as a new *Muscari* subg. *Pulchella*, consisting of seven species, including *M. latifolium*, *M. bourgaei*, *M. kerkis*, and the type species, *M. pulchellum*. However, in their plastid tree, *M.* subg. *Pulchella* is paraphyletic. *Muscari pulchellum* is sister to *M. kerkis*, which in turn is sister to *Leopoldia neumannii*. The remaining *M.* subg. *Pulchella* species are instead sister to *M.* subg. *Leopoldia*. We recovered a similar relationship when analysing the combined plastid tree, which incorporates both our data and that of Böhnert & al. (2023) (suppl. Fig. S8). This suggests that while the Muscari N2 and P2 clades are currently monophyletic, they may not remain so with the inclusion of the remaining *M.* subg. *Pulchella* species. Therefore, depending on the analyses, we will continue to refer to the second *M.* subg. *Muscari* clade as Muscari N2 and P2.

Böhnert & al. (2023) suggest that *Muscari* subg. *Pulchella* occupies an intermediate position between *M.* subg. *Leopoldia* and subg. *Muscari*, based on its nested placement in their phylogenies and similar perianth morphology. However, our phylogenies (Figs. 4, 5, 6) and NANUQ species network analysis (Fig. 7) do not support *M.* subg. *Pulchella* as an intermediate lineage between these subgenera. Specifically, the NANUQ species network reveals little to no gene flow between the Muscari N1 and N2 clades, and *M.* subg. *Leopoldia* (Leopoldia clade) (Fig. 7). This suggests that the similar features which *M.* subg. *Pulchella* shares with *Muscari* s.str. and *M.* subg. *Leopoldia* (Böhnert & al. 2023), might instead have arisen from the distant common ancestor of these subgenera (symplesiomorphy) and highlights the problematic use of floral morphology in delimiting taxa in *Muscari* s.l. Instead, substantial gene flow is observed among the Muscari N2 clade, *M.* subg. *Pseudomuscari* (Pseudomuscari clade) and subg. *Muscarimia* (Muscarimia clade), which is plausible given the shared distributions of species within these groups. Further sampling and investigation would be required to fully untangle these relationships.

Cytonuclear discordance, along with low nuclear concordance scores, often indicates hybridisation between taxa (Rieseberg & Soltis, 1991; Fu & al., 2022; Stull & al., 2023). This discordance is seen between species in *Muscari* subg. *Leopoldia* and subg. *Muscari* (suppl. Fig. S7). These subgenera frequently co-occur and flower at the same time (Davis & Stuart, 1980, 1984; Suárez-Santiago & Blanca, 2013), while also sharing many floral morphological features including a constricted perianth and mostly scentless flowers. Such shared characters suggest that species in these subgenera might be part of a pollinator guild (Fenster & al., 2004), in which they have morphologically similar flowers to attract a common pollinator (Newman & al., 2014; Faure & al., 2022) and therefore an increased chance of interspecies gene flow. Such an understanding of pollination syndrome is key to evaluating the likelihood of gene flow as a plausible cause for discordance in the phylogenetic trees recovered (Mallet, 2005; S. Xu & al., 2011; Goulet & al., 2017). Although limited research has been conducted on plant-pollinator interactions within *Muscari* s.l., Canale & al. (2014) report that *M. comosum* (subg. *Leopoldia*) is pollinated by a wide range of pollinators, including Hymenoptera (mostly generalist solitary bees) and Diptera (bee flies), which also pollinate other species in *M.* subg. *Muscari* including *M. neglectum*. Despite this, there are no records of hybridisation between these subgenera and the NANUQ network (Fig. 7) supports the lack of gene flow. However, hybridisation due to overlapping historical ranges, has been reported in Ledebouriinae (Asparagaceae, Scilloideae) between *Drimiopsis* Lindl. & Paxton and *Ledebouria* Roth (Howard & al., 2022, 2023) and during the early diversification of Nolinoideae (Asparagaceae) (Ji & al., 2023). Such an understanding of pollination syndrome is key to evaluating the likelihood of gene flow as a plausible cause for discordance in the phylogenetic trees recovered.

Therefore, the lack of evidence towards hybridisation suggests that the discordance between the nuclear and

plastome phylogenies is likely a result of incomplete lineage sorting (Meleshko & al., 2021; L.L. Xu & al., 2021; McLay & al., 2023; Zhang & al., 2024). Due to its biparentally inherited nature, nuclear DNA has double the effective population size when compared the uniparentally inherited plastome DNA (Crosby & Smith, 2012). Larger effective population sizes often result in longer allele coalescence times (Nordborg & Krone, 2002), thereby increasing the likelihood of incomplete lineage sorting. Furthermore, if species have experienced rapid speciation events, which could be reflected by the short internal branches in our *Muscari* phylogenies, incomplete lineage sorting might be the cause of conflict due to the insufficient time available for alleles to converge within a population (Degnan & Rosenberg, 2009; Angelis & Dos Reis, 2015).

The incongruity between our two nuclear analyses could be attributed to the nature of the nuclear regions employed. Nuclear ribosomal cistrons exist in numerous copies throughout the genome but are susceptible to homogenisation via concerted evolution, resulting in the cistrons evolving together, rather than independently (Ohta, 1983). In contrast, low-copy nuclear gene data encompass an array of individual nuclear loci drawn from across the nuclear genome, each evolving independently (Peterson & al., 2012).

Within our sampling of *Muscari* subg. *Leopoldia* we have multiple accessions of five different species: *M. comosum*, *M. massayanum*, *M. mirum*, *M. spreitzenhoferi* (Heldr.) Vierh., and *M. weissii*. Of these, only *M. mirum* and *M. spreitzenhoferi* are consistently resolved as clades in our analyses. Neither *M. massayanum* nor *M. weissii* are recovered as monophyletic in the plastome and nuclear ribosomal cistron analyses (Figs. 5, 6). *Muscari massayanum* is endemic to Turkey with a disjunct southern and eastern distribution (Davis & Stuart, 1984). The population around Adana in the south is where the type of *M. massayanum* originated. A recent taxonomic assessment by Eker (2021) separated the eastern population of *M. massayanum* around Gümüshane as a distinct species, *M. erzincanicum* Eker, differing from *M. massayanum* in capsule morphology and pedicel length. Therefore, the sample MMASS, collected from Gümüshane, under the name *M. massayanum*, is likely to be *M. erzincanicum*, while sample M32_2, collected in Adana, is *M. massayanum*. Böhnert & al. (2023) in their plastid analyses recovered *M. massayanum* in *M.* subg. *Muscarimia*

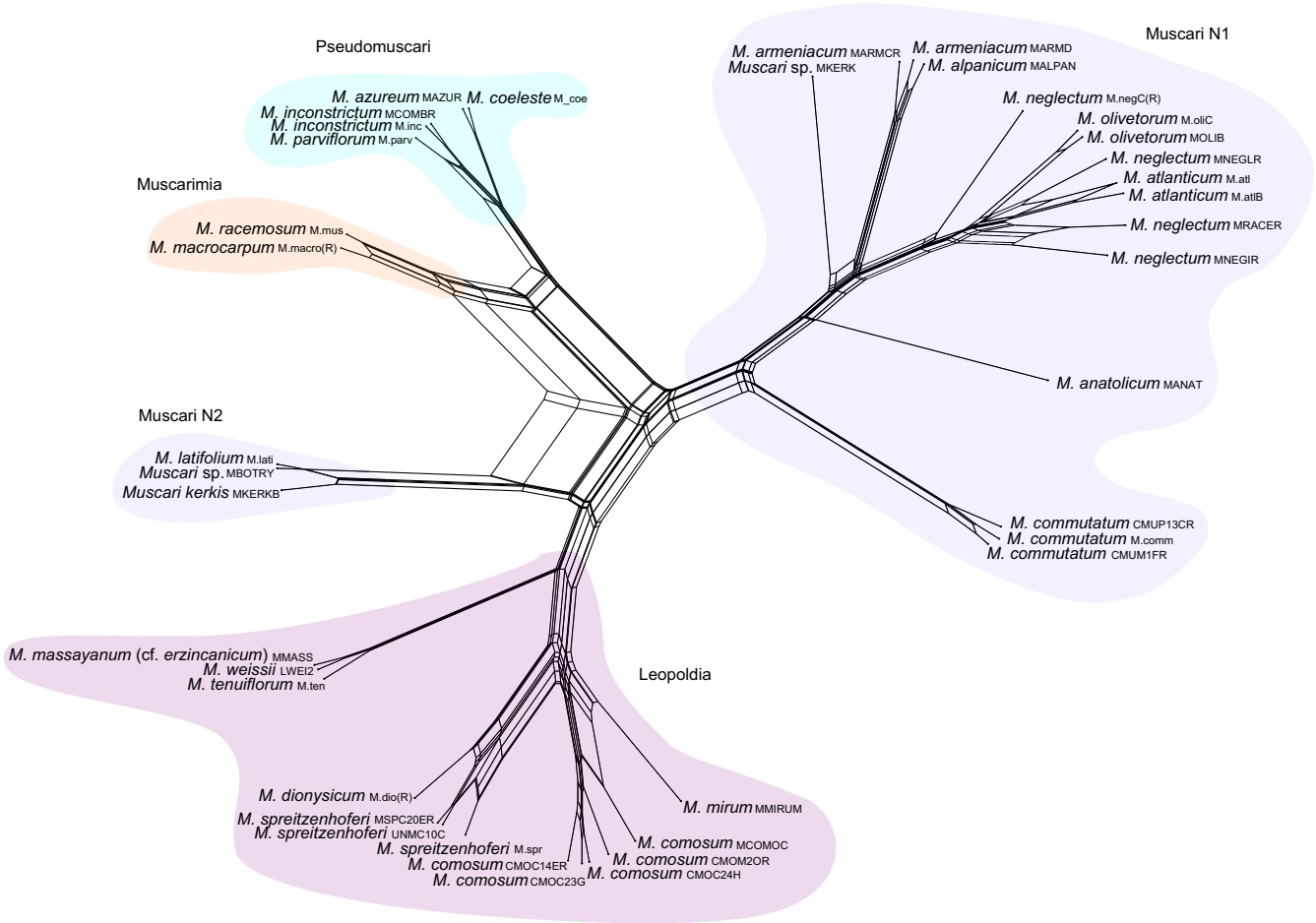

Fig. 7. A species network inferred from 284 low-copy nuclear gene trees of *Muscari* s.l. using NANUQ (alpha = 1e-06, beta = 0.95) as implemented in MSCquartets. Colours denote subgenera.

while their ddRAD nuclear analyses recovered it in *M*. subg. *Leopoldia*. However, no detailed locality notes are provided for their accession of *M. massayanum* for comparison.

Muscari weissii is distributed throughout southwest Turkey, Greece, and the Aegean Islands (Davis & Stuart, 1984; Dimopoulos & al., 2016). Our samples of *M. weissii* were collected from Antalya, Turkey (M12_3) and Ioannina, Northwestern Greece (LWEI2), thus matching the reported distribution of the species. The Greek *M. weissii* (LWEI2) is consistently recovered as sister to *M. massayanum* (MMASS, cf. *erzincanicum*), in all three analyses. However, the placement of the Turkish sample of *M. weissii* (M12_3) (not included in the low-copy nuclear gene analyses) differs between the plastome analyses in which it is sister to the Turkish *M. massayanum* (M32_2) (Fig. 5) congruent with Dizkirici & al. (2019), and our nuclear ribosomal cistron analyses in which it emerges as sister to *M. comosum* (Fig. 6). Hybridisation has been reported between *M. weissii* and *M. comosum* (Davis & Stuart, 1984), potentially accounting for the clustering of *M. weissii* (M12_3) with *M. comosum* in the nuclear ribosomal cistron tree. Additionally, *Muscari dionysicum* is a recognised synonym of *M. weissii*. However, material received under the name *M. dionysicum* (M.dio(R)), was consistently recovered as sister to *M. spreitzenhoferi* across all analyses—an unexpected placement that may reflect misidentification.

Furthermore, all three analyses recovered the Iberian endemic *Muscari matritense* either sister to or within the highly polymorphic and widespread *M. comosum*. Although both species are morphologically very similar, *M. matritense* was separated from *M. comosum* based upon karyological differences (Ruiz Rejón & al., 1985). However, considering the marked genetic and morphological polymorphisms (Davis & Stuart, 1980, 1984) exhibited by *M. comosum* (López Alonso & Reguera, 1986; Rejon & al., 1987; Garrido-Ramos & al., 1998), along with the close phylogenetic relationship with *M. matritense*, it is possible that *M. matritense* represents morphological variation within *M. comosum* instead of being a separate species.

Within *Muscari* subg. *Muscari* our analyses recovered the Spanish endemic *M. olivetorum* either sister to *M. atlanticum* and the highly polymorphic and widespread *M. neglectum* in the nuclear trees (Figs. 4, 6) or within *M. neglectum* in the plastome tree (Fig. 5). Suárez-Santiago & al. (2007), in their nuclear ITS analyses of Spanish *Muscari*, reported a similar placement of *M. olivetorum* as found in our nuclear analyses. The authors suggest a possible hybrid origin of *M. olivetorum* with *M. neglectum* and *M. baeticum* Blanca & al. as parents. The three species have overlapping distribution further supporting the hypothesis of hybrid origin (Suárez-Santiago & Blanca, 2013). However, we could not obtain *M. baeticum* for our investigation and therefore could not further explore the possible hybrid origin of *M. olivetorum*.

Another notable placement is the varying position of *M. commutatum* across all three phylogenies. It has been traditionally placed within *M*. subg. *Muscari*, on account of its dense conical raceme of blue, black, or violet fertile oblong-urceolate flowers and an inconspicuous apical ring of sterile flowers. Both our low-copy nuclear gene analysis (Muscari N1 clade, Fig. 4) and the ddRAD analysis by Böhnert & al. (2023) place *M. commutatum* within *M*. subg. *Muscari*, but sister to all other species in the subgenus. This differentiation is reflected in the NANUQ species network (Fig. 7). However, the plastome analysis places *M. commutatum* (Muscari P4 clade) outside *M*. subg. *Muscari* sister to *M. mirum* (Leopoldia P3 clade) (Fig. 5), while our nuclear ribosomal cistron analysis places it within *M*. subg. *Muscari* (Muscari clade) but on a long, poorly supported branch (Fig. 6). Thus, the placement of *M. commutatum* within *Muscari* s.l. remains uncertain and warrants further investigation, as also suggested by Böhnert & al. (2023).

Taxonomic remarks. — The recovery of the Muscari N2 and P2 clades, separate from the remainder of *Muscari* subg. *Muscari* is consistent with Böhnert & al. (2023), who recognised a *M*. subg. *Pulchella* for this group. Böhnert & al. (2023) found this to be a monophyletic group in their ddRAD analysis but not in their plastid sequence analysis, which had slightly different sampling. This suggests the monophyly of *M*. subg. *Pulchella* is sensitive both to data type and taxon sampling and we would consider it premature to recognise this as a distinct taxon. However, we were not able to include *M. pulchellum*, the type of *M*. subg. *Pulchella*, in our sampling.

A pragmatic alternative, that recognises a consistently stable part of the low-copy nuclear and plastid phylogenies, is to merge *Muscari* subg. *Leopoldia* and subg. *Muscari* into one large *M*. subg. *Muscari* (0.99 LPP, 1.00 PP respectively), that would result in *Muscari* s.l. containing three subgenera as previously suggested by Tynkevich & al. (2023). However, this larger *M*. subg. *Muscari* would be paraphyletic in the nuclear ribosomal cistron analysis, with support at 0.89 PP.

Additionally, the NANUQ species network (Fig. 7) revealed limited gene flow between *Muscari* subg. *Leopoldia* (Leopoldia clade) and subg. *Muscari* (Muscari N1and N2 clades). Therefore, merging these subgenera may not accurately represent their evolutionary history and would unite two groups with significantly different inflorescence morphologies into a single subgenus, which cannot itself be distinguished based on morphological characteristics.

The differences among phylogenies highlight that the subgeneric delineation of *Muscari* s.l. can vary depending on the molecular data and taxon sampling strategy used, thereby making it challenging to establish a robust and stable subgeneric taxonomic treatment of the genus. More comprehensive taxon sampling is needed, particularly for the low-copy nuclear gene analysis. This approach, when combined with non-floral traits such as seed morphology, may better represent the observed evolutionary patterns. The use of seed morphology has already proven useful in studies of Turkish species of *Muscari* s.l. (Eroğlu & al., 2021).

Since conducting this research, an Asparagaceae-specific bait kit (Asparagaceae1726; Bentz & Leebens-Mack, 2024) has been developed. The use of this bait kit, along with

increased taxon sampling, may provide higher numbers of phylogenetically informative nuclear genes, which could aid in resolving the subgeneric delimitations within *Muscari* s.l.

Nomenclatural change. — The results of this paper are consistent with those of Böhnert & al. (2023) in recognising a Pseudomuscari clade, which includes the majority of species that were included in in Garbari's (1970, 1973) and Stuart's (1970) original species list for the genus *Pseudomuscari* and *Muscari* subg. *Pseudomuscari*.

Böhnert & al. (2023) indicate that *M.* subg. *Pseudomuscari* was validly published by Stuart (1985) based on Losinskaya's invalidly published "*M.* sect. *Pseudomuscari*" (Losina-Losinskaya, 1935). However, this is predated by Stuart's (1970) valid publication of the subgenus. Stuart (1970) designated *Muscari pallens* as the type of the subgenus, selecting it from among the species included by Losina-Losinskaya in her "sect. *Pseudomuscari*" (Losina-Losinskaya, 1935).

Our results (suppl. Fig. S8) and those of Böhnert & al. (2023) show that *Muscari pallens* belongs in *M.* subg. *Muscari*, rendering Stuart's subgenus a synonym of the type subgenus. Additionally, this is corroborated by a review of the corresponding herbarium specimen of *M. pallens* which we deemed to have been correctly identified (see Appendix 1, Böhnert & al., 2023).

Garbari & Greuter (1970) in describing the genus *Pseudomuscari* designated *M. azureum* as the type. Böhnert & al. (2023) likewise state that the type of "*M.* subg. *Pseudomuscari* (Losinsk.) D.C.Stuart" is *M. azureum*. The existence of the validly published *M.* subg. *Pseudomuscari* D.C.Stuart prevents the recombination of Gabari & Greuter's genus as a subgenus. It is also the case that it is not possible to conserve Stuart's subgenus with a new type (i.e., *M. azureum*) (Turland & al., 2018: Art. 14.1) and it is therefore necessary to publish a new subgeneric name for the Pseudomuscari clade. The new subgeneric name has no implications for *Pseudomuscari* Gabari & Greuter, which remains the correct name for the group of species in the Pseudomuscari clade when treated at generic rank. Our choice of '*Paramuscari*' reflects the position of this taxon sister to other elements of *Muscari* it has traditionally been grouped with.

Muscari subg. ***Paramuscari*** H.R.Hall, Culham, Könyves & J.C.David, **subg. nov.** – Type: *Muscari azureum* Fenzl.

Description. – Bulbs obovoid. Annual slender roots. Leaves 2–4(–6), linear to oblong lanceolate, flaccid to erect. Lax or dense racemes of pale to dark blue flowers, often with dark blue central markings. The fertile flowers are shortly to oblong campanulate. Spring flowering species have weakly to non-constricted perianths, while the autumn-flowering *Muscari parviflorum* is constricted. Perianth teeth concolorous with rest of the perianth. Sterile flowers are few, either pedicellate or sessile.

All species listed below were included in Garbari's (1970, 1973) and Stuart's (1970) original species list for the genus *Pseudomuscari* and subgenus *Pseudomuscari*. Not all species mentioned were studied; therefore, the asterisk (*) indicates the material included in this investigation.

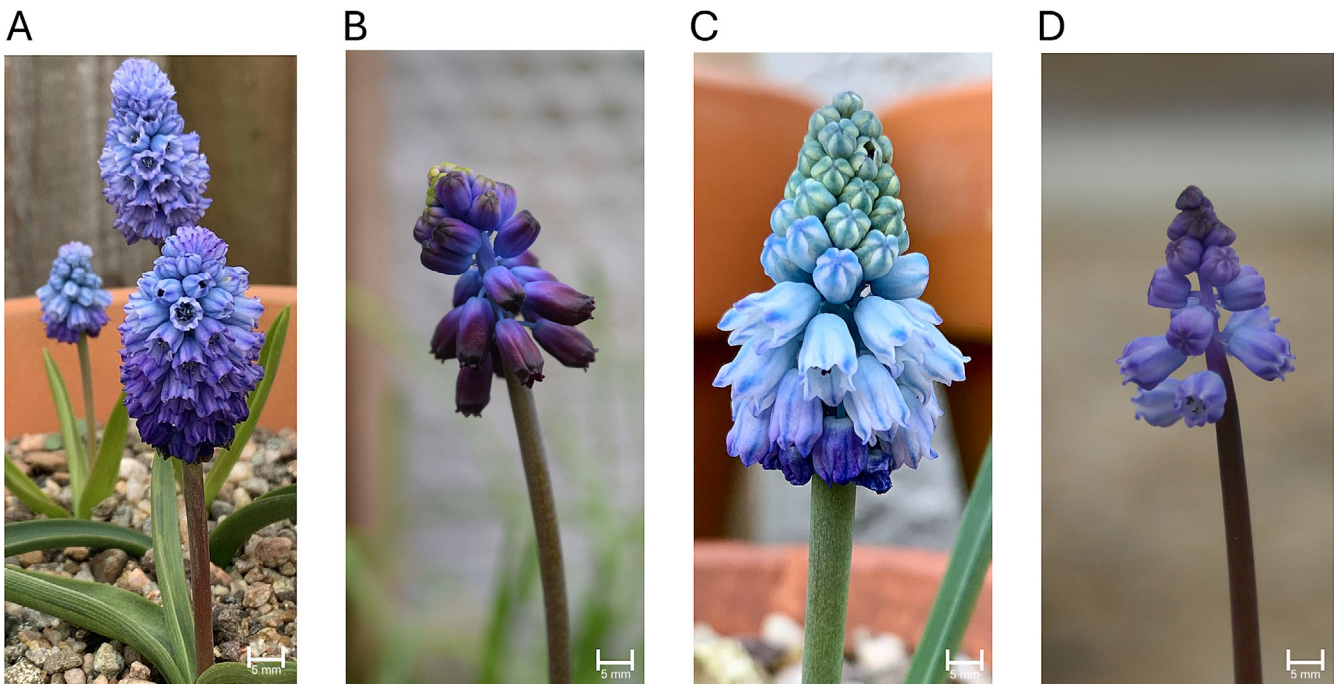

Fig. 8. Four of the species included in *Muscari* subg. *Paramuscari*: **A**, *M. azureum*; **B**, *M. inconstrictum*; **C**, *M. coeleste*; **D**, *M. parviflorum*. — Photos: A & C, Debbie Amor (Gardeneasta); B & D, John David.

Species included in *Muscari* subg. *Paramuscari* (Fig. 8)

**Muscari azureum* Fenzl, Index Seminum [Vienna] 1858: 4. 1858 ≡ *Pseudomuscari azureum* (Fenzl) Garbari & Greuter in Taxon 19: 334. 1970.

* *Muscari coeleste* Fomin in Věstn. Tiflissk. Bot. Sada 9: 11. 1908 ≡ *Pseudomuscari coeleste* (Fomin) Garbari in Atti Soc. Tosc. Sci. Nat., ser. B, 77: 112. 1970.
= *Hyacinthella turkewiczii* Woronow in Bot. Mater. Gerb. Glavn. Bot. Sada R.S.F.S.R. 5: 88. 1924 ≡ *Muscari turkewiczii* (Woronow) Losinsk. in Komarov, Fl. URSS 4: 420. 1935 ≡ *Pseudomuscari turkewiczii* (Woronow) Garbari in Atti Soc. Tosc. Sci. Nat., ser. B, 77: 112. 1970.

* *Muscari inconstrictum* Rech.f. in Ark. Bot., ser. 2, 2: 314. 1952 ≡ *Pseudomuscari inconstrictum* (Rech.f.) Garbari in Atti Soc. Tosc. Sci. Nat., ser. B, 77: 112. 1970.

* *Muscari parviflorum* Desf., Fl. Atlant. 1: 309. 1798.

* *Muscari pseudomuscari* (Boiss. & Buhse) Wendelbo in Notes Roy. Bot. Gard. Edinburgh 38: 433. 1980 ≡ *Bellevalia pseudomuscari* Boiss. & Buhse in Boissier, Diagn. Pl. Orient., ser. 2, 4: 110. 1859.
= *Muscari chalusicum* D.C.Stuart in Lily Year-Book 30: 125. 1966 ≡ *Pseudomuscari chalusicum* (D.C.Stuart) Garbari in Atti Soc. Tosc. Sci. Nat., ser. B, 77: 112. 1970.

Species excluded from *Muscari* subg. *Paramuscari* (Fig. 9)

Muscari acutifolium Boiss., Fl. Orient. 5(1): 300. 1882 ≡ *Pseudomuscari actutifolium* (Boiss.) Garbari in Atti Soc. Tosc. Sci. Nat., ser. B, 77: 112. 1970.
= *Hyacinthus paradoxus* Fisch. & C.A.Mey, Index Seminum [St. Petersburg (Petropolitanus)] 1: 30. 1835 ≡ *Muscari paradoxum* (Fisch. & C.A.Mey.) K.Koch in Linnaea 22: 253. 1849 ≡ *Bellevalia paradoxa* (Fisch. & C.A.Mey.) Boiss., Fl. Orient. 5(1): 308. 1882 ≡ *Pseudomuscari paradoxum* (Fisch. & C.A.Mey.) Garbari in Atti Soc. Tosc. Sci. Nat., ser. B, 77: 112. 1970. — Genus *Bellevalia*.

Muscari apertum Freyn & Conrath in Bull. Herb. Boissier 4: 194. 1896 ≡ *Pseudomuscari apertum* (Freyn & Conrath) Garbari in Atti Soc. Tosc. Sci. Nat., ser. B, 77: 112. 1970.
= *Muscari armeniacum* H.J.Veitch in Garden (London, 1871–1927) 1: 687. 1872. — Subgenus *Muscari*.

Muscari coeruleum Losinsk. in Komarov, Fl. URSS 4: 412, 745. 1935 ≡ *Pseudomuscari coeruleum* (Losinsk.) Garbari in Atti Soc. Tosc. Sci. Nat., ser. B, 77: 112. 1970. — Subgenus *Muscari*.

* *Muscari forniculatum* Fomin in Věstn. Tiflissk. Bot. Sada 9: 12. 1908 ≡ *Bellevalia forniculata* (Fomin) Delaunay in Věstn. Tiflissk. Bot. Sada, n.s., 1: 30. 1922 ≡ *Pseudomuscari forniculatum* (Fomin) Garbari in Atti Soc. Tosc. Sci. Nat., ser. B, 77: 112. 1970. — Genus *Bellevalia*.

* *Muscari discolor* Boiss. & Hausskn. in Boissier, Fl. Orient. 5(1): 300. 1882. — Subgenus *Muscari*.

Muscari pallens (M.Bieb.) Fisch., Cat. Jard. Gorenki, ed. 2: 9. 1812 ≡ *Hyacinthus pallens* M.Bieb., Fl. Taur.-Caucas. 1: 283. 1808 ≡ *Pseudomuscari pallens* (M.Bieb.) Garbari in Atti Soc. Tosc. Sci. Nat., ser. B, 77: 112. 1970. — Subgenus *Muscari*.

■ CONCLUSIONS

Using low-copy nuclear gene, plastome, and nuclear ribosomal cistron data, we have uncovered significant incongruence in the subgeneric delineation of *Muscari* s.l., particularly evident within *M.* subg. *Leopoldia* and subg. *Muscari*. This incongruence may be attributed to complex evolutionary processes such as incomplete lineage sorting and hybridisation, which together make the establishment of a stable subgeneric taxonomic treatment of the genus difficult when based solely on molecular data. By considering such phylogenetic patterns in the context of evolutionary events, morphology, and ecology, we have begun to enhance our understanding of the evolutionary complexities within this genus of widely cultivated plants. Future studies should aim to achieve a broader sampling across the taxonomic and

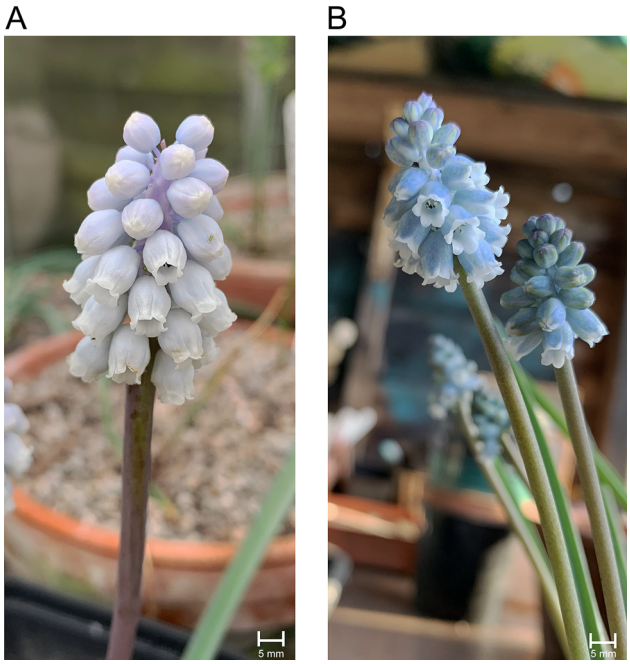

Fig. 9. Two species of *Muscari* s.l. that have been included in *Muscari* subg. *Pseudomuscari* on the grounds of floral morphology but now included in *M.* subg. *Muscari*: **A**, *M. pallens*; **B**, *M. coeruleum*. — Photos: Debbie Amor (Gardeneasta).

geographic breadth of *Muscari* s.l., in addition to a more thorough analyses of both nuclear and organellar genomes, as the delineation of *Muscari* s.l. appears to be sensitive to both taxon and molecular data sampling. Such investigations will be essential for more in-depth empirical testing of evolutionary history. Additionally, through our review of nomenclatural literature, we have identified the need for a new name and delimitation for *M*. subg. *Pseudomuscari* due to the placement of *M. pallens*, the type of *M*. subg. *Pseudomuscari* sensu Stuart, within *M*. subg. *Muscari*.

■ AUTHORS CONTRIBUTIONS

AC, KK and JD, conceptualised the study. HH and AC conducted fieldwork. HH, JB and AD conducted DNA extractions. HH analysed the data and HH, AC, KK, JD, and JB interpreted the results. HH drafted the manuscript, and all authors revised the manuscript.

■ ACKNOWLEDGMENTS

The *Muscari* samples from Turkey, related to the DNA samples provided by Dizkirici & al. (2019), were collected as part of the project TUBITAK 114Z736, in which Ayten Tekpinar is the principal investigator. We thank Mesut Pinar for collecting the samples. Additionally, we thank RHS Wisley, Gothenburg Botanical Garden, Cambridge University Botanic Garden, Herbarium of the University of Malaga (MGC), Royal Botanic Garden Edinburgh, Botanical Garden of the University of Fribourg, and Debbie Amor (Gardeneasta) for providing leaf material for this study and Debbie Amor (Gardeneasta) for providing photos of *Muscari* subg. *Pseudomuscari/Paramuscari*. We also thank the Greek and Spanish (Andalusia, and Balearic Islands) governments for providing plant collection permits. We thank J. Garcia Sanchez, F. Soriguer, N. Hidalgo, D. Bautista and M. Rocio of MGC for collecting *Muscari* in Spain. We thank the Hardy Plant Society and the Stoke Poges, Wexham and Fulmer Horticultural Society for fieldwork funding. We also acknowledge the help of Eleanor Lansley, who as part of the Undergraduate Research Opportunities Programme at the University of Reading, helped with some of the data handling and processing of herbarium specimens. Additionally, we acknowledge the help of Evita Kypraki, who aided us in obtaining the Greek collecting permits and accompanied HH and AC on fieldwork. Finally, we would like to thank the University of Reading and Royal Horticultural Society for providing the funding for this study as part of the Ph.D. studies of HH.

■ LITERATURE CITED

Ali, S.S., Yu, Y., Pfosser, M. & Wetschnig, W. 2012. Inferences of biogeographical histories within subfamily Hyacinthoideae using S-DIVA and Bayesian binary MCMC analysis implemented in RASP (Reconstruct Ancestral State in Phylogenies). *Ann. Bot. (Oxford)* 109: 95–107. https://doi.org/10.1093/aob/mcr274

Alipour, S., Majidi, R. & Eker, I. 2024. *Muscari zagricum* (Asparagaceae, Scilloideae), a unique new species from Iran. *Phytotaxa* 652: 133–141. https://doi.org/10.11646/PHYTOTAXA.652.2.5

Allman, E.S., Baños, H. & Rhodes, J.A. 2019. NANUQ: A method for inferring species networks from gene trees under the coalescent model. *Algorithms Molec. Biol.* 14: 24. https://doi.org/10.1186/s13015-019-0159-2

Allman, E., Banos, H., Mitchell, J., Wicke, K. & Rhodes, J. 2024. MSCquartets: Analyzing Gene Tree Quartets under the Multi-Species Coalescent. *R package version* 3.0. Available from: https://CRAN.R-project.org/package=MSCquartets

Angelis, K. & Dos Reis, M. 2015. The impact of ancestral population size and incomplete lineage sorting on Bayesian estimation of species divergence times. *Curr. Zool.* 61: 874–885. https://doi.org/10.1093/czoolo/61.5.874

Baker, J.G. 1871. A revision of the genera and species of the herbaceous capsular gamophyllous Liliaceae. *J. Linn. Soc., Bot.* 11: 349–436. https://doi.org/10.1111/j.1095-8339.1870.tb00068.x

Bánki, O., Roskov, Y., Döring, M., Ower, G., Hernández Robles, D.R., Plata Corredor, C.A., Stjernegaard Jeppesen, T., Örn, A., Pape, T., Hobern, D., Garnett, S., Little, H., DeWalt, R.E., Ma, K., Miller, J., Orrell, T., Aalbu, R., Abbott, J., Adlard, R. & al. 2025. Catalogue of Life, version 2025-02-13. Catalogue of Life, Amsterdam, Netherlands. https://doi.org/10.48580/dgnfb

Bentz, P.C. & Leebens-Mack, J. 2024. Developing Asparagaceae1726: An Asparagaceae-specific probe set targeting 1726 loci for Hyb-Seq and phylogenomics in the family. *Applic. Pl. Sci* 12: e11597. https://doi.org/10.1002/aps3.11597

Böhnert, T., Neumann, M., Quandt, D. & Weigend, M. 2023. Phylogeny based generic reclassification of *Muscari* sensu lato (Asparagaceae) using plastid and genomic DNA. *Taxon* 72: 261–277. https://doi.org/10.1002/tax.12864

Bolger, A.M., Lohse, M. & Usadel, B. 2014. Trimmomatic: A flexible trimmer for Illumina sequence data. *Bioinformatics* 30: 2114–2120. https://doi.org/10.1093/bioinformatics/btu170

Borowiec, M.L. 2016. AMAS: A fast tool for alignment manipulation and computing of summary statistics. *PeerJ* 4: e1660. https://doi.org/10.7717/peerj.1660

Buerki, S., Jose, S., Yadav, S.R., Goldblatt, P., Manning, J.C. & Forest, F. 2012. Contrasting biogeographic and diversification patterns in two mediterranean-type ecosystems. *PLoS ONE* 7(6): e39377. https://doi.org/10.1371/journal.pone.0039377

Canale, A., Benelli, G. & Benvenuti, S. 2014. First record of insect pollinators visiting *Muscari comosum* (L.) Miller (Liliaceae-Hyacinthaceae), an ancient Mediterranean food plant. *Pl. Biosyst.* 148: 889–894. https://doi.org/10.1080/11263504.2013.863810

Capella-Gutiérrez, S., Silla-Martínez, J.M. & Gabaldón, T. 2009. trimAl: A tool for automated alignment trimming in large-scale phylogenetic analyses. *Bioinformatics* 25: 1972–1973. https://doi.org/10.1093/bioinformatics/btp348

Chan, P.P., Lin, B.Y., Mak, A.J. & Lowe, T.M. 2021. tRNAscan-SE 2.0: Improved detection and functional classification of transfer RNA genes. *Nucl. Acids Res.* 49: 9077–9096. https://doi.org/10.1093/nar/gkab688

Crosby, K. & Smith, D.R. 2012. Does the mode of plastid inheritance influence plastid genome architecture? *PLoS ONE* 7(9): e46260. https://doi.org/10.1371/journal.pone.0046260

Darriba, D., Taboada, G.L., Doallo, R. & Posada, D. 2012. jModelTest 2: More models, new heuristics and parallel computing. *Nature Meth.* 9: 772. https://doi.org/10.1038/nmeth.2109

Davis, P.H. & Stuart, D.C. 1980. *Muscari* Miller. Pp. 46–49 in: Tutin, T.G., Heywood, V.H., Burges, N.A., Moore, D.M., Valentine, D.H., Walters, S.M. & Webb, D.A. (eds.), *Flora Europaea*, vol. 5. Cambridge: Cambridge University Press.

Davis, P.H. & Stuart, D.C. 1984. *Muscari* Miller. Pp. 245–263 in: Davis, P.H. (ed.), *Flora of Turkey*, vol. 8. Edinburgh: Edinburgh University Press.

De Vere, N., Rich, T.C.G., Ford, C.R., Trinder, S.A., Long, C., Moore, C.W., Satterthwaite, D., Davies, H., Allainguillaume, J., Ronca, S., Tatarinova, T., Garbett, H., Walker, K. & Wilkinson, M.J. 2012. DNA barcoding the native flowering plants and conifers of Wales. *PLoS ONE* 7(6): e37945. https://doi.org/10.1371/journal.pone.0037945

Degnan, J.H. & Rosenberg, N.A. 2009. Gene tree discordance, phylogenetic inference and the multispecies coalescent. *Trends Ecol. Evol.* 24: 332–340. https://doi.org/10.1016/j.tree.2009.01.009

Dierckxsens, N., Mardulyn, P. & Smits, G. 2017. NOVOPlasty: De novo assembly of organelle genomes from whole genome data. *Nucl. Acids Res.* 45: e18. https://doi.org/10.1093/nar/gkw955

Dimopoulos, P., Raus, T., Bergmeier, E., Constantinidis, T., Iatrou, G., Kokkini, S., Strid, A. & Tzanoudakis, D. 2016. Vascular plants of Greece: An annotated checklist; Supplement. *Willdenowia* 46: 301–347. https://doi.org/10.3372/wi.46.46303

Dizkirici, A., Yigit, O., Pinar, M. & Eroglu, H. 2019. Molecular phylogeny of *Muscari* (Asparagaceae) inferred from cpDNA sequences. *Biológia (Bratislava)* 74: 205–214. https://doi.org/10.2478/s11756-018-00164-0

Dodsworth, S., Pokorny, L., Johnson, M.G., Kim, J.T., Maurin, O., Wickett, N.J., Forest, F. & Baker, W.J. 2019. Hyb-Seq for flowering plant systematics. *Trends Pl. Sci.* 24: 887–891. https://doi.org/10.1016/j.tplants.2019.07.011

Doğu, S. & Uysal, T. 2019. *Muscari savranii* (Asparagaceae), a new species from central Anatolia, Turkey. *Phytotaxa* 402: 155–164. https://doi.org/10.11646/phytotaxa.402.3.3

Edgar, R.C. 2004. MUSCLE: Multiple sequence alignment with high accuracy and high throughput. *Nucl. Acids Res.* 32: 1792–1797. https://doi.org/10.1093/nar/gkh340

Eker, İ. 2019a. *Muscari fatmacereniae* (Asparagaceae, Scilloideae), a new species from Southern Anatolia. *Phytotaxa* 397: 99–106. https://doi.org/10.11646/phytotaxa.397.1.10

Eker, İ. 2019b. *Muscari pamiryigidii* (Asparagaceae, Scilloideae), a new species from northwestern Anatolia. *Phytotaxa* 408: 255–266. https://doi.org/10.11646/phytotaxa.408.4.2

Eker, İ. 2021. What is *Muscari massayanum* and what is not? Second species born of confusion: *Muscari erzincanicum* (Asparagaceae, Scilloideae), a new species from Turkey. *Phytotaxa* 487: 41–55. https://doi.org/10.11646/phytotaxa.487.1.3

Eker, İ. & Yildirim, H. 2021. *Muscari inundatum* (Asparagaceae, Scilloideae), a new species from southern Anatolia. *Phytotaxa* 484: 181–194. https://doi.org/10.11646/phytotaxa.484.2.3

Eker, İ., Duman, H. & Yildirim, H. 2020. *Muscari muglaensis* (Asparagaceae, Scilloideae), a new species from southwestern Anatolia. *Phytotaxa* 475: 267–278. https://doi.org/10.11646/phytotaxa.475.4.4

Eroğlu, H., Karaismailoğlu, M.C., Pinar, S.M. & Fidan, M. 2021. Seed micromorphology and anatomy of 36 *Muscari* (Asparagaceae) taxa from Turkey with notes on their systematic importance. *Acta Bot. Croat.* 80: 146–157. https://doi.org/10.37427/BOTCRO-2021-015

Faure, J., Martén-Rodríguez, S., Clark, J.L. & Joly, S. 2022. The level of pollination specialization affects the relationship between the shape of flowers and the bills of their hummingbird pollinators in Antillean Gesneriaceae. *Int. J. Pl. Sci.* 183: 193–204. https://doi.org/10.1086/718221

Fenster, C.B., Armbruster, W.S., Wilson, P., Dudash, M.R. & Thomson, J.D. 2004. Pollination syndromes and floral specialization. *Annual Rev. Ecol. Evol. Syst.* 35: 375–403. https://doi.org/10.1146/annurev.ecolsys.34.011802.132347

Folk, R.A., Gaynor, M.L., Engle-Wrye, N.J., O'Meara, B.C., Soltis, P.S., Soltis, D.E., Guralnick, R.P., Smith, S.A., Grady, C.J. & Okuyama, Y. 2023. Identifying climatic drivers of hybridization with a new ancestral niche reconstruction method. *Syst. Biol.* 72: 856–873. https://doi.org/10.1093/sysbio/syad018

Fu, R., Zhu, Y., Liu, Y., Feng, Y., Lu, R. Sen, Li, Y., Li, P., Kremer, A., Lascoux, M. & Chen, J. 2022. Genome-wide analyses of introgression between two sympatric Asian oak species. *Nature Ecol. Evol.* 6: 924–935. https://doi.org/10.1038/s41559-022-01754-7

Garbari, F. 1970. *Pseudomuscari*, nuovo genere di Liliaceae. *Atti Soc. Tosc. Sci. Nat. Pisa, Mem.* 77: 112.

Garbari, F. 1973. Note sul genere «*Pseudomuscari*» (Liliaceae). *Webbia* 27: 369–381. https://doi.org/10.1080/00837792.1973.10669979

Garbari, F. & Greuter, W. 1970. On the taxonomy and typification of *Muscari* Miller (Liliaceae) and allied genera, and on the typification of generic names. *Taxon* 19: 329–335. https://doi.org/10.2307/1219056

Garnett, G.J.L., Könyves, K., Bilsborrow, J., David, J. & Culham, A. 2020. The complete plastome of *Hyacinthoides non-scripta* (L.) Chouard ex Rothm. (Asparagaceae). *Mitochondrial DNA, B*, 5: 1003–1004. https://doi.org/10.1080/23802359.2020.1720543

Garrido-Ramos, M.A., Jamilena, M., De La Herrán, R., Ruiz Rejón, C., Camacho, J.P.M. & Ruiz Rejón, M. 1998. Inheritance and fitness effects of a pericentric inversion and a supernumerary chromosome segment in *Muscari comosum* (Liliaceae). *Heredity* 80: 724–731. https://doi.org/10.1046/j.1365-2540.1998.00344.x

Gonçalves, D.J.P., Simpson, B.B., Ortiz, E.M., Shimizu, G.H. & Jansen, R.K. 2019. Incongruence between gene trees and species trees and phylogenetic signal variation in plastid genes. *Molec. Phylogen. Evol.* 138: 219–232. https://doi.org/10.1016/j.ympev.2019.05.022

Goulet, B.E., Roda, F. & Hopkins, R. 2017. Hybridization in plants: Old ideas, new techniques. *Pl. Physiol. (Lancaster)* 173: 65–78. https://doi.org/10.1104/pp.16.01340

Greiner, S., Lehwark, P. & Bock, R. 2019. OrganellarGenomeDRAW (OGDRAW) version 1.3.1: Expanded toolkit for the graphical visualization of organellar genomes. *Nucl. Acids Res.* 47: W59–W64. https://doi.org/10.1093/nar/gkz238

Guindon, S., Dufayard, J.F., Lefort, V., Anisimova, M., Hordijk, W. & Gascuel, O. 2010. New algorithms and methods to estimate maximum-likelihood phylogenies: Assessing the performance of PhyML 3.0. *Syst. Biol.* 59: 307–321. https://doi.org/10.1093/sysbio/syq010

Hoang, D.T., Chernomor, O., von Haeseler, A., Minh, B.Q. & Vinh, L.S. 2018. UFBoot2: Improving the ultrafast bootstrap approximation. *Molec. Biol. Evol.* 35: 518–522. https://doi.org/10.1093/molbev/msx281

Howard, C.C., Crowl, A.A., Harvey, T.S. & Cellinese, N. 2022. Peeling back the layers: First phylogenomic insights into the Ledebouriinae (Scilloideae, Asparagaceae). *Molec. Phylogen. Evol.* 169: 107430. https://doi.org/10.1016/j.ympev.2022.107430

Howard, C.C., Nanyeni, L., Mollel, N., Chuba, D., Zuntini, A.R., Malakasi, P., Harvey, T.S. & Cellinese, N. 2023. From southern Africa and beyond: Historical biogeography of a monocotyledonous bulbous geophyte. *J. Biogeogr.* 50: 1623–1638. https://doi.org/10.1111/jbi.14627

Huson, D.H. 1998. SplitsTree: Analyzing and visualizing evolutionary data. *Bioinformatics* 14: 68–73. https://doi.org/10.1093/bioinformatics/14.1.68

Huson, D.H. & Bryant, D. 2024. The SplitsTree App: interactive analysis and visualization using phylogenetic trees and networks. *Nature Meth.* 21: 1773–1774. https://doi.org/10.1038/s41592-024-02406-3

Jang, T.S., Emadzade, K., Parker, J., Temsch, E.M., Leitch, A.R., Speta, F. & Weiss-Schneeweiss, H. 2013. Chromosomal diversification and karyotype evolution of diploids in the cytologically diverse genus *Prospero* (Hyacinthaceae). *B. M. C. Evol. Biol.* 13. https://doi.org/10.1186/1471-2148-13-136

Ji, Y., Landis, J.B., Yang, J., Wang, S., Zhou, N., Luo, Y. & Liu, H. 2023. Phylogeny and evolution of Asparagaceae subfamily Nolinoideae: New insights from plastid phylogenomics. *Ann. Bot. (Oxford)* 131: 301–312. https://doi.org/10.1093/aob/mcac144

Jin, J.J., Yu, W. Bin, Yang, J.B., Song, Y., Depamphilis, C.W., Yi, T.S. & Li, D.Z. 2020. GetOrganelle: A fast and versatile

toolkit for accurate de novo assembly of organelle genomes. *Genome Biol.* 21: 241. https://doi.org/10.1186/s13059-020-02154-5

Johnson, M.G., Gardner, E.M., Liu, Y., Medina, R., Goffinet, B., Shaw, A.J., Zerega, N.J.C. & Wickett, N.J. 2016. HybPiper: Extracting coding sequence and introns for phylogenetics from high-throughput sequencing reads using target enrichment. *Applic. Pl. Sci.* 4: 1600016. https://doi.org/10.3732/apps.1600016

Johnson, M.G., Pokorny, L., Dodsworth, S., Botigué, L.R., Cowan, R.S., Devault, A., Eiserhardt, W.L., Epitawalage, N., Forest, F., Kim, J.T., Leebens-Mack, J.H., Leitch, I.J., Maurin, O., Soltis, D.E., Soltis, P.S., Wong, G.K., Baker, W.J. & Wickett, N.J. 2019. A universal probe set for targeted sequencing of 353 nuclear genes from any flowering plant designed using k-Medoids clustering. *Syst. Biol.* 68: 594–606. https://doi.org/10.1093/sysbio/syy086

Junier, T. & Zdobnov, E.M. 2010. The Newick utilities: High-throughput phylogenetic tree processing in the Unix shell. *Bioinformatics* 26: 1669–1670. https://doi.org/10.1093/bioinformatics/btq243

Kalyaanamoorthy, S., Minh, B.Q., Wong, T.K.F., von Haeseler, A. & Jermiin, L.S. 2017. ModelFinder: Fast model selection for accurate phylogenetic estimates. *Nature Meth.* 14: 587–589. https://doi.org/10.1038/nmeth.4285

Karlén, T. 1984. *Muscari pulchellum* (Liliaceae) and associated taxa in Greece and W Turkey. *Willdenowia* 14: 89–118.

Katoh, K. & Standley, D.M. 2013. MAFFT multiple sequence alignment software version 7: Improvements in performance and usability. *Molec. Biol. Evol.* 30: 772–780. https://doi.org/10.1093/molbev/mst010

Katoh, K., Misawa, K., Kuma, K.I. & Miyata, T. 2002. MAFFT: A novel method for rapid multiple sequence alignment based on fast Fourier transform. *Nucl. Acids Res.* 30: 3059–3066. https://doi.org/10.1093/nar/gkf436

Kayiran, S.D., Özhatay, N. & Kaya, E. 2019. *Muscari tauricum* (Asparagaceae, Scilloideae), a new species from Turkey. *Phytotaxa* 399: 109–118. https://doi.org/10.11646/phytotaxa.399.2.1

Laslett, D. 2004. ARAGORN, a program to detect tRNA genes and tmRNA genes in nucleotide sequences. *Nucl. Acids Res.* 32: 11–16. https://doi.org/10.1093/nar/gkh152

Li, H. & Durbin, R. 2009. Fast and accurate short read alignment with Burrows–Wheeler transform. *Bioinformatics* 25: 1754–1760. https://doi.org/10.1093/bioinformatics/btp324

Liu, J., Lindstrom, A.J. & Gong, X. 2022. Towards the plastome evolution and phylogeny of *Cycas* L. (Cycadaceae): Molecular-morphology discordance and gene tree space analysis. *B. M. C. Pl. Biol.* 22: 116. https://doi.org/10.1186/s12870-022-03491-2

López Alonso, D. & Reguera, L.P. 1986. Population structure and pattern of geographic variation in *Muscari comosum* along its range of distribution. *Genetica* 78: 39–49. https://doi.org/10.1007/BF00058673

Losina-Losinskaya, A. 1935. *Muscari*. Pp. 412–422 in: Komarov, V.L. (ed.), *Flora URSS*, vol. 4. Leningrad: Editio Academiae scientiarum URSS. [in Russian]

Mai, U. & Mirarab, S. 2018. TreeShrink: Fast and accurate detection of outlier long branches in collections of phylogenetic trees. *B. M. C. Genomics* 19: 272. https://doi.org/10.1186/s12864-018-4620-2

Mallet, J. 2005. Hybridization as an invasion of the genome. *Trends Ecol. Evol.* 20: 229–237. https://doi.org/10.1016/j.tree.2005.02.010

McLay, T.G.B., Birch, J.L., Gunn, B.F., Ning, W., Tate, J.A., Nauheimer, L., Joyce, E.M., Simpson, L., Schmidt-Lebuhn, A.N., Baker, W.J., Forest, F. & Jackson, C.J. 2021. New targets acquired: Improving locus recovery from the Angiosperms353 probe set. *Applic. Pl. Sci.* 9: e11420. https://doi.org/10.1002/aps3.11420

McLay, T.G.B., Fowler, R.M., Fahey, P.S., Murphy, D.J., Udovicic, F., Cantrill, D.J. & Bayly, M.J. 2023. Phylogenomics reveals extreme gene tree discordance in a lineage of dominant trees: Hybridization, introgression, and incomplete lineage sorting blur deep evolutionary relationships despite clear species groupings in *Eucalyptus* subgenus *Eudesmia*. *Molec. Phylogen. Evol.* 187: 107869. https://doi.org/10.1016/j.ympev.2023.107869

Meleshko, O., Martin, M.D., Korneliussen, T.S., Schröck, C., Lamkowski, P., Schmutz, J., Healey, A., Piatkowski, B.T., Shaw, A.J., Weston, D.J., Flatberg, K.I., Szövényi, P., Hassel, K. & Stenøien, H.K. 2021. Extensive genome-wide phylogenetic discordance is due to incomplete lineage sorting and not ongoing introgression in a rapidly radiated bryophyte genus. *Molec. Biol. Evol.* 38: 2750–2766. https://doi.org/10.1093/molbev/msab063

Minh, B.Q., Schmidt, H.A., Chernomor, O., Schrempf, D., Woodhams, M.D., von Haeseler, A., Lanfear, R. & Teeling, E. 2020a. IQ-TREE 2: New models and efficient methods for phylogenetic inference in the genomic era. *Molec. Biol. Evol.* 37: 1530–1534. https://doi.org/10.1093/molbev/msaa015

Minh, B.Q., Hahn, M.W. & Lanfear, R. 2020b. New methods to calculate concordance factors for phylogenomic datasets. *Molec. Biol. Evol.* 37(9): 2727–2733. https://doi.org/10.1093/molbev/msaa106

Newman, E., Manning, J. & Anderson, B. 2014. Matching floral and pollinator traits through guild convergence and pollinator ecotype formation. *Ann. Bot. (Oxford)* 113: 373–384. https://doi.org/10.1093/aob/mct203

Nicolle, D., Ritter, M.K., Jones, R.C., Phillips, G.P., French, M.E., Cumming, R. & Bell, S.A.J. 2025. The genus problem – *Eucalyptus* as a model system for minimising taxonomic disruption. *Taxon* 74: 495–506. https://doi.org/10.1002/tax.13240

Nordborg, M. & Krone, S.M. 2002. Separation of time scales and convergence to the coalescent in structured populations. Pp. 194–232 in: Slatkin, M. & Veuille, M. (eds.), *Modern developments in theoretical population genetics: The legacy of Gustave Malecot*. Oxford: Oxford University Press. https://doi.org/10.1093/oso/9780198599623.003.0012

Ohta, T. 1983. On the evolution of multigene families. *Theor. Populat. Biol.* 23: 216–240. https://doi.org/10.1016/0040-5809(83)90015-1

Peterson, B.K., Weber, J.N., Kay, E.H., Fisher, H.S. & Hoekstra, H.E. 2012. Double digest RADseq: An inexpensive method for de novo SNP discovery and genotyping in model and non-model species. *PLoS ONE* 7: e37135. https://doi.org/10.1371/journal.pone.0037135

Pfosser, M. & Speta, F. 1999. Phylogenetics of Hyacinthaceae based on plastid DNA sequences. *Ann. Missouri Bot. Gard.* 86: 852–875. https://doi.org/10.2307/2666172

Rambaut, A., Drummond, A.J., Xie, D., Baele, G. & Suchard, M.A. 2018. Posterior summarization in Bayesian phylogenetics using Tracer 1.7. *Syst. Biol.* 67: 901–904. https://doi.org/10.1093/sysbio/syy032

Ranwez, V., Douzery, E.J.P., Cambon, C., Chantret, N. & Delsuc, F. 2018. MACSE v2: Toolkit for the alignment of coding sequences accounting for frameshifts and stop codons. *Molec. Biol. Evol.* 35: 2582–2584. https://doi.org/10.1093/molbev/msy159

Rejon, C.R., Lozano, R. & Rejon, M.R. 1987. Genetic variability in *Muscari comosum* L. (Liliaceae). II. Characterization and effects of the polymorphic variants of chromosome 2 on chiasmata formation. *Genome* 29: 695–701. https://doi.org/10.1139/g87-119

Rhodes, J.A., Baños, H., Mitchell, J.D. & Allman, E.S. 2021. MSCquartets 1.0: Quartet methods for species trees and networks under the multispecies coalescent model in R. *Bioinformatics* 37: 1766–1768. https://doi.org/10.1093/bioinformatics/btaa868

Rieseberg, L.H. & Soltis, D.E. 1991. Phylogenetic consequences of cytoplasmic gene flow in plants. *Evol. Trends Pl.* 5: 65–84.

Robbins, E.H.J. & Kelly, S. 2023. The evolutionary constraints on angiosperm chloroplast adaptation. *Genome Biol. Evol.* 15: evad101. https://doi.org/10.1093/gbe/evad101

Ronquist, F., Teslenko, M., Van Der Mark, P., Ayres, D.L., Darling, A., Höhna, S., Larget, B., Liu, L., Suchard, M.A. & Huelsenbeck, J.P. 2012. MrBayes 3.2: Efficient Bayesian phylogenetic inference and model choice across a large model space. *Syst. Biol.* 61: 539–542. https://doi.org/10.1093/sysbio/sys029

Roudsari, L.J., Vaezi, J. & Jafari, A. 2025. Phylogenetic relationships of *Bellevalia* species (Asparagaceae), inferred from morphology and molecular systematics. *Phytotaxa* 700: 196–204. https://doi.org/10.11646/phytotaxa.700.2.3

Ruiz Rejón, M., Pascual, L., Ruiz Rejón, C., Valdés, B. & Oliver, J.L. 1985. A new species of *Muscari* subgenus *Leopoldia* from the Iberian Peninsula. *Biochem. Syst. Ecol.* 13: 239–250. https://doi.org/10.1016/0305-1978(85)90032-8

Sayyari, E. & Mirarab, S. 2016. Fast coalescent-based computation of local branch support from quartet frequencies. *Molec. Biol. Evol.* 33: 1654–1668. https://doi.org/10.1093/MOLBEV/MSW079

Shi, C., Hu, N., Huang, H., Gao, J., Zhao, Y.J. & Gao, L.Z. 2012. An improved chloroplast DNA extraction procedure for whole plastid genome sequencing. *PLoS ONE* 7: e31468. https://doi.org/10.1371/journal.pone.0031468

Speta, F. 1998. Hyacinthaceae. Pp. 261–285 in: Kubitzky, K. (ed.), *The families and genera of vascular plants*, vol. 3. Berlin, Heidelberg: Springer. https://doi.org/10.1007/978-3-662-03533-7_35

Straub, S.C.K., Parks, M., Weitemier, K., Fishbein, M., Cronn, R.C. & Liston, A. 2012. Navigating the tip of the genomic iceberg: Next-generation sequencing for plant systematics. *Amer. J. Bot.* 99: 349–364. https://doi.org/10.3732/ajb.1100335

Stuart, D.C. 1970. Chromosome numbers in the genus *Muscari* Mill. *Notes Roy. Bot. Gard. Edinburgh* 30: 189–196.

Stuart, D.C. 1985. *Muscari*. Pp. 126–135 in: Townsend, C.C. & Guest, E. (eds.), *Flora of Iraq*, vol. 8. Baghdad: Ministry of Agriculture & Agrarian Reform.

Stull, G.W., Pham, K.K., Soltis, P.S. & Soltis, D.E. 2023. Deep reticulation: The long legacy of hybridization in vascular plant evolution. *Plant J.* 114: 743–766. https://doi.org/10.1111/tpj.16142

Suárez-Santiago, V.N. & Blanca, G. 2013. *Muscari* Mill. Pp. 171–184 in: *Flora Iberica*, vol. 20. Madrid: Real Jardín Botánico, CSIC.

Suárez-Santiago, V.N., Salinas, M.J., Romero-García, A.T., Garrido-Ramos, M.A., De La Herrán, R., Ruiz-Rejón, C., Ruiz-Rejón, M. & Blanca, G. 2007. Polyploidy, the major speciation mechanism in *Muscari* subgenus *Botryanthus* in the Iberian Peninsula. *Taxon* 56: 1171–1184. https://doi.org/10.2307/25065910

Tillich, M., Lehwark, P., Pellizzer, T., Ulbricht-Jones, E.S., Fischer, A., Bock, R. & Greiner, S. 2017. GeSeq – versatile and accurate annotation of organelle genomes. *Nucl. Acids Res.* 45: W6–W11. https://doi.org/10.1093/nar/gkx391

Turland, N.J., Wiersema, J.H., Barrie, F.R., Greuter, W., Hawksworth, D.L., Herendeen, P.S., Knapp, S., Kusber, W.-H., Li, D.-Z., Marhold, K., May, T.W., McNeill, J., Monro, A.M., Prado, J., Price, M.J. & Smith, G.F. (eds.) 2018. *International Code of Nomenclature for algae, fungi, and plants (Shenzhen Code) adopted by the Nineteenth International Botanical Congress Shenzhen, China, July 2017*. Regnum Vegetabile 159. Glashütten: Koeltz Botanical Books. https://doi.org/10.12705/Code.2018

Tutin, T.G., Heywood, V.H., Burges, N.A., Moore, D.M., Valentine, D.H., Walters, S.M. & Webb, D.A. 1980. *Flora Europaea*, vol. 5, *Alismataceae to Orchidaceae (Monocotyledones)*. Cambridge: Cambridge University Press.

Twyford, A.D. & Ennos, R.A. 2012. Next-generation hybridization and introgression. *Heredity* 108: 179–189. https://doi.org/10.1038/hdy.2011.68

Tynkevich, Y.O., Boychuk, S.V., Shelyfist, A.Y., Chorney, I.I. & Volkov, R.A. 2023. Molecular phylogeny and genetic diversity of Carpathian members of the genus *Muscari* inferred from plastid DNA sequences. *Cytol. & Genet.* 57: 387–398. https://doi.org/10.3103/S0095452723050079

Uysal, T., Aksoy, A., Bozkurt, M. & Ertuğrul, K. 2022. A new grape hyacinth from East Anatolia (Turkey) *Muscari vanensis* (subgenus *Botryanthus*). *Phytotaxa* 536: 53–71. https://doi.org/10.11646/phytotaxa.536.1.3

Walker, J.F., Walker-Hale, N., Vargas, O.M., Larson, D.A. & Stull, G.W. 2019. Characterizing gene tree conflict in plastome-inferred phylogenies. *PeerJ* 7: e7747. https://doi.org/10.7717/peerj.7747

Weitemier, K., Straub, S.C.K., Cronn, R.C., Fishbein, M., Schmickl, R., McDonnell, A. & Liston, A. 2014. Hyb-Seq: Combining target enrichment and genome skimming for plant phylogenomics. *Applic. Pl. Sci.* 2: 1400042. https://doi.org/10.3732/apps.1400042

Xu, L.L., Yu, R.M., Lin, X.R., Zhang, B.W., Li, N., Lin, K., Zhang, D.Y. & Bai, W.N. 2021. Different rates of pollen and seed gene flow cause branch-length and geographic cytonuclear discordance within Asian butternuts. *New Phytol.* 232: 388–403. https://doi.org/10.1111/nph.17564

Xu, S., Schlüter, P.M., Scopece, G., Breitkopf, H., Gross, K., Cozzolino, S. & Schiestl, F.P. 2011. Floral isolation is the main reproductive barrier among closely related sexually deceptive orchids. *Evolution (Lancaster)* 65: 2606–2620. https://doi.org/10.1111/j.1558-5646.2011.01323.x

Zhang, C., Rabiee, M., Sayyari, E. & Mirarab, S. 2018. ASTRAL-III: Polynomial time species tree reconstruction from partially resolved gene trees. *B. M. C. Bioinf.* 19: 153. https://doi.org/10.1186/s12859-018-2129-y

Zhang, X., Sun, Y., Landis, J.B., Lv, Z., Shen, J., Zhang, H., Lin, N., Li, L., Sun, J., Deng, T., Sun, H. & Wang, H. 2020. Plastome phylogenomic study of Gentianeae (Gentianaceae): Widespread gene tree discordance and its association with evolutionary rate heterogeneity of plastid genes. *B. M. C. Pl. Biol.* 20: 340. https://doi.org/10.1186/s12870-020-02518-w

Zhang, Z.Z., Liu, G. & Li, M. 2024. Incomplete lineage sorting and gene flow within *Allium* (Amaryllidaceae). *Molec. Phylogen. Evol.* 195: 108054. https://doi.org/10.1016/j.ympev.2024.108054

Appendix 1. Species included in this study with their corresponding voucher information (sample code, geographic origin, collector, collection number, herbarium code), and GenBank accession numbers (whole plastome; trimmed nuclear ribosomal cistron; SRA). A dash (–) indicates missing sequences. Sequences newly generated for this study are marked by an asterisk (*); samples with sample code starting with M, e.g., M14_2, are from Dizkirici & al. (2019). SRA data available under BioProject Code: PRJNA1208223.

Bellevalia forniculata (Fomin) Delaunay, B_forB2, Cultivated material, *John David s.n.* (WSY), PQ210127*, PQ129957*, SRR32756938*, ***Bellevalia hyacinthoides*** (Bertol.) K.Perss. & Wendelbo, B_hya2, Cultivated material, *Kálmán Könyves & John David s.n.* (WSY), PQ210128*, PQ129958*, SRR32756937*, ***Muscari adilii*** M.B.Güner & H.Duman, M18_3, Turkey, *Mesut Pinar s.n.* (VANF), PQ210146*, PQ129976*, SRR32756916*, ***Muscari alpanicum*** Schchian, MALPAN, Cultivated material, *John David s.n.* (WSY), PQ210178*, PQ130008*, SRR32756891*, ***Muscari anatolicum*** Cowley & Özhatay, M29_2, Turkey, *Mesut Pinar s.n.* (VANF), PQ210155*, PQ129985*, SRR32756905*, ***Muscari anatolicum*** Cowley & Özhatay, MANAT, Greece, *Jimmy Persson JP 87-77* (GBG), PQ210179*,

Appendix 1. Continued.

PQ130009*, SRR32756890*, ***Muscari armeniacum*** H.J.Veitch, M11_1, Turkey, *Mesut Pinar s.n.* (VANF), PQ210141*, PQ129971*, SRR32756921*, ***Muscari armeniacum*** H.J.Veitch, MARMCR, Turkey (not vouchered), PQ210180*, PQ130010*, SRR32756889*, ***Muscari armeniacum*** H.J.Veitch, MARMD, Cultivated material, *s.coll. s.n.* (RBGE), PQ210181*, PQ130011*, SRR32756888*, ***Muscari atlanticum*** Boiss. & Reut., M.atl, Spain, *García-Sánchez & F. Soriguer s.n.* (MGC), PQ210167*, PQ129997*, SRR32756932*, ***Muscari atlanticum*** Boiss. & Reut., M.atlB, Spain, *García-Sánchez & F. Soriguer s.n.* (MGC), PQ210168*, PQ129998*, SRR32756931*, ***Muscari aucheri*** Baker, MAUCH, Turkey (not vouchered), PQ210182*, PQ130012*, SRR32756887*, ***Muscari azureum*** Fenzl, M25_3, Turkey, *Mesut Pinar s.n.* (VANF), PQ210151*, PQ129981*, SRR32756909*, ***Muscari azureum*** Fenzl, MAZUR, Cultivated material, *John David s.n.* (WSY), PQ210183*, PQ130013*, SRR32756886*, ***Muscari babachii*** Eker & Koyuncu, M39_1, Turkey, *Mesut Pinar s.n.* (VANF), PQ210162*, PQ129992*, SRR32756897*, ***Muscari bourgaei*** Baker, M26_3, Turkey, *Mesut Pinar s.n.* (VANF), PQ210152*, PQ129982*, SRR32756908*, ***Muscari caucasicum*** Baker, M35_1, Turkey, *Mesut Pinar s.n.* (VANF), PQ210161*, PQ129991*, SRR32756898*, ***Muscari coeleste*** Fomin, M_coe, Cultivated material, *Kálmán Könyves & John David s.n.* (WSY), PQ210165*, PQ129995*, SRR32756936*, ***Muscari coeleste*** Fomin, M20_1, Turkey, *Mesut Pinar s.n.* (VANF), PQ210147*, PQ129977*, SRR32756913*, ***Muscari coeleste*** Fomin, M20_3, Turkey, *Mesut Pinar s.n.* (VANF), PQ210148*, PQ129978*, SRR32756912*, ***Muscari commutatum*** Guss., CMUM1FR, Greece, *Hannah Hall, Alastair Culham, Evita Kypraki MLH1* (RNG), PQ210133*, PQ129963*, SRR32756882*, ***Muscari commutatum*** Guss., CMUP13CR, Greece, *Hannah Hall, Alastair Culham, Evita Kypraki PPH13* (RNG), PQ210134*, PQ129964*, SRR32756871*, ***Muscari commutatum*** Guss., M.comm, Cultivated material, *Kálmán Könyves & John David s.n.* (WSY), PQ210169*, PQ129999*, SRR32756930*, ***Muscari comosum*** Mill., CMOC14ER, Greece, *Hannah Hall, Alastair Culham, Evita Kypraki, David Pearce CRH14* (RNG), PQ210129*, PQ129959*, SRR32756926*, ***Muscari comosum*** Mill., CMOC23G, Greece, *Hannah Hall, Alastair Culham, Evita Kypraki, David Pearce CRH23* (RNG), PQ210130*, PQ129960*, SRR32756915*, ***Muscari comosum*** Mill., CMOC24H, Greece, *Hannah Hall, Alastair Culham, Evita Kypraki CRH24* (RNG), PQ210131*, PQ129961*, SRR32756904*, ***Muscari comosum*** Mill., CMOM2OR, Greece, *Hannah Hall, Alastair Culham, Evita Kypraki MLH2* (RNG), PQ210132*, PQ129962*, SRR32756893*, ***Muscari comosum*** Mill., M5_2, Turkey, *Mesut Pinar s.n.* (VANF), PQ210139*, PQ129969*, SRR32756894*, ***Muscari comosum*** Mill., MCOMOC, Spain, *García-Sánchez, F. Soriguer & M. Recio s.n.* (MGC), PQ210184*, PQ130014*, SRR32756885*, ***Muscari cycladicum*** P.H.Davis & D.C.Stuart, L_cyc1, Cultivated material, *Kálmán Könyves & John David s.n.* (WSY), PQ210135*, PQ129965*, SRR32756860*, ***Muscari dionysicum*** Rech.f., M.dio(R), Cultivated material, *Kálmán Könyves & John David s.n.* (WSY), PQ210170*, PQ130000*, SRR32756929*, ***Muscari discolor*** Boiss. & Hausskn. ex Boiss., M2_4, Turkey, *Mesut Pinar s.n.* (VANF), PQ210138*, PQ129968*, SRR32756914*, ***Muscari erdalii*** Özhatay & Demirci, M40_2, Turkey, *Mesut Pinar s.n.* (VANF), PQ210163*, PQ129993*, SRR32756896*, ***Muscari grandifolium*** Baker, M_gra, Cultivated material, *Kálmán Könyves & John David s.n.* (WSY), PQ210166*, PQ129996*, SRR32756935*, ***Muscari inconstrictum*** Rech.f., M.inc, Cultivated material, *John David s.n.* (WSY), PQ210171*, PQ130001*, SRR32756934*, ***Muscari inconstrictum*** Rech.f., MCOMBR, Iraq, *Henrick, Gerben, Django EGO.IQ.146* (GBG), –, –, SRR32756866*, ***Muscari kerkis*** Karlén, MKERKB, Cultivated matierial, *Debbie Amor s.n.* (RNG), –, –, SRR32756865*, ***Muscari latifolium*** J.Kirk., M.lati, Cultivated material, *John David s.n.* (WSY), PQ210172*, PQ130002*, SRR32756928*, ***Muscari latifolium*** J.Kirk., M22_2, Turkey, *Mesut Pinar s.n.* (VANF), PQ210149*, PQ129979*, SRR32756911*, ***Muscari longipes*** Boiss., M31_3, Turkey, *Mesut Pinar s.n.* (VANF), PQ210157*, PQ129987*, SRR32756902*, ***Muscari macbeathianum*** Kit Tan, M30_1, Turkey, *Mesut Pinar s.n.* (VANF), PQ210156*, PQ129986*, SRR32756903*, ***Muscari macrocarpum*** Sweet, M.macro(R), Cultivated material, *John David s.n.* (WSY), PQ210173*, PQ130003*, SRR32756927*, ***Muscari macrocarpum*** Sweet, M14_2, Turkey, *Mesut Pinar s.n.* (VANF), PQ210144*, PQ129974*, SRR32756918*, ***Muscari massayanum*** C.Grunert, M32_2, Turkey, *Mesut Pinar s.n.* (VANF), PQ210158*, PQ129988*, SRR32756901*, ***Muscari massayanum*** (cf. ***erzincanicum***), MMASS, Turkey, *Kummert, Pasche & Pirc K2P 0512* (GBG), PQ210185*, PQ130016*, SRR32756883*, ***Muscari matritense*** Ruíz Rejón, Pascual, C.Ruíz Rejón, Valdés & J.L.Oliv., MMATRI, Spain, *F. Soriguer s.n.* (MGC), PQ210186*, PQ130017*, SRR32756881*, ***Muscari microstomum*** P.H.Davis & D.C.Stuart, M28_2, Turkey, *Mesut Pinar s.n.* (VANF), PQ210154*, PQ129984*, SRR32756906*, ***Muscari mirum*** Speta, M34_2, Turkey, *Mesut Pinar s.n.* (VANF), PQ210160*, PQ129990*, SRR32756899*, ***Muscari mirum*** Speta, MMIRUM, Cultivated matierial, *Debbie Amor s.n.* (RNG), PQ210187*, PQ130018*, SRR32756880*, ***Muscari neglectum*** Guss. ex Ten. & Sangiov, M.negC(R), Cultivated material, *John David s.n.* (WSY), PQ210175*, PQ130005*, SRR32756933*, ***Muscari neglectum*** Guss. ex Ten. & Sangiov, M1_4, Turkey, *Mesut Pinar s.n.* (VANF), PQ210137*, PQ129967*, SRR32756922*, ***Muscari neglectum*** Guss. ex Ten. & Sangiov, MNEGER, Greece, *s.coll. s.n.* (RBGE), PQ210188*, PQ130019*, SRR32756879*, ***Muscari neglectum*** Guss. ex Ten. & Sangiov, MNEGLR, Greece (not vouchered), PQ210189*, PQ130020*, SRR32756878*, ***Muscari neglectum*** Guss. ex Ten. & Sangiov, MRACER, Austria (not vouchered), PQ210192*, PQ130023*, SRR32756875*, ***Muscari neglectum*** Guss. ex Ten. & Sangiov, MNEGIR, Cultivated material, *Kálmán Könyves & John David s.n.* (WSY), –, –, SRR32756864*, ***Muscari olivetorum*** Blanca, Ruíz Rejón & Suár.-Sant., M.oliC, Spain, *García-Sánchez & F. Soriguer s.n.* (MGC), PQ210176*, PQ130006*, SRR32756924*, ***Muscari olivetorum*** Blanca, Ruíz Rejón & Suár.-Sant., MOLIB, Spain, *García-Sánchez & F. Soriguer s.n.* (MGC), PQ210190*, PQ130021*, SRR32756877*, ***Muscari olivetorum*** Blanca, Ruíz Rejón & Suár.-Sant., MOLIVR, Spain, *García-Sánchez & F. Soriguer s.n.* (MGC), PQ210191*, PQ130022*, SRR32756876*, ***Muscari parviflorum*** Desf., M42_2, Turkey, *Mesut Pinar s.n.* (VANF), PQ210164*, PQ129994*, SRR32756895*, ***Muscari parviflorum**** Desf., M.parv, Cultivated material, *Kálmán Könyves & John David s.n.* (WSY), –, –, SRR32756861*, ***Muscari pseudomuscari*** (Boiss. & Buhse) Wendelbo, P_cha, Cultivated material, *John David s.n.* (WSY), PQ210194*, PQ130025*, SRR32756873*, ***Muscari racemosum*** Mill., M.mus, Cultivated material, *Kálmán Könyves & John David s.n.* (WSY), PQ210174*, PQ130004*, SRR32756925*, ***Muscari racemosum*** Mill., M13_1, Turkey, *Mesut Pinar s.n.* (VANF), PQ210143*, PQ129973*, SRR32756919*, ***Muscari sandrasicum*** Karlén, M24_2, Turkey, *Mesut Pinar s.n.* (VANF), PQ210150*, PQ129980*, SRR32756910*, ***Muscari serpentinicum*** Yıldırım, Altıoğlu & Pirhan, M33_2, Turkey, *Mesut Pinar s.n.* (VANF), PQ210159*, PQ129989*, SRR32756900*, ***Muscari sivrihisardaghlarensis*** Yıldırımlı & B.Selvi, M16_1, Turkey, *Mesut Pinar s.n.* (VANF), PQ210145*, PQ129975*, SRR32756917*, ***Muscari* sp.**, MKERK, Greece, *Arne Strid AS 54666* (GBG), PQ210198*, PQ130015*, SRR32756884*, ***Muscari* sp.**, MBOTRY, Switzerland (not vouchered), –, –, SRR32756867*, ***Muscari spreitzenhoferi*** (Heldr. ex Osterm.) H.R.Wehrh., MSPC20ER, Greece, *Hannah Hall, Alastair Culham, Evita Kypraki CRH20* (RNG), PQ210193*, PQ130024*, SRR32756874*, ***Muscari spreitzenhoferi*** (Heldr. ex Osterm.) H.R.Wehrh., UNMC10C, Greece, *Hannah Hall, Alastair Culham, Evita Kypraki CRH10* (RNG), PQ210197*, PQ130028*, SRR32756869*, ***Muscari spreitzenhoferi*** (Heldr. ex Osterm.) H.R.Wehrh., M.spr, Cultivated material, *Kálmán Könyves & John David s.n.* (WSY), –, –, SRR32756868*, ***Muscari tenuiflorum*** Tausch, M.ten, Cultivated material, *Kálmán Könyves & John David s.n.* (WSY), PQ210177*, PQ130007*, SRR32756923*, ***Muscari turcicum*** Uysal, Ertuğrul & Dural, M27_1, Turkey, *Mesut Pinar s.n.* (VANF), PQ210153*, PQ129983*, SRR32756907*, ***Muscari vuralii*** Bağcı & Doğu, M9_2, Turkey, *Mesut Pinar s.n.* (VANF), PQ210140*, PQ129970*, SRR32756892*, ***Muscari weissii*** Freyn, LWEI2, Greece (not vouchered), PQ210136*, PQ129966*, SRR32756859*, ***Muscari weissii*** Freyn, M12_3, Turkey, *Mesut Pinar s.n.* (VANF), PQ210142*, PQ129972*, SRR32756920*, ***Othocallis siberica*** (Haw.) Speta, S_sib1, Cultivated material, *John David s.n.* (WSY), PQ210196*, PQ130027*, SRR32756870*, ***Othocallis siberica*** (Haw.) Speta, SSIB, Cultivated material, *Kálmán Könyves & John David s.n.* (WSY), –, –, SRR32756862*, ***Schnarfia messeniaca*** (Boiss.) Speta, S_mes1, Cultivated material, *John David s.n.* (WSY), PQ210195*, PQ130026*, SRR32756872*, ***Schnarfia messeniaca*** (Boiss.) Speta, SMP7CR, Greece, *Hannah Hall, Alastair Culham, Evita Kypraki PPH7* (RNG), –, –, SRR32756863*.